

Supporting Information to

Palladium Alkyl Complexes with a Formazanate Ligand: Synthesis, Structure and Reactivity

Francesca Milocco,^{†,‡} Folkert de Vries,^{†,‡} Anna Dall'Anese,[‡] Vera Rosar,^{**} Ennio Zangrando,[‡]
Edwin Otten^{*,†} and Barbara Milani^{*,‡}

[‡] Dipartimento di Scienze Chimiche e Farmaceutiche, Università di Trieste, Via Licio Giorgieri 1, 34127 Trieste, Italy

[†] Stratingh Institute for Chemistry, University of Groningen, Nijenborgh 4, 9747 AG Groningen, The Netherlands

^{*}Current address: Department of Chemistry and Biochemistry, University of Bern, Freiestrasse 3, 3012 Bern, Switzerland

Contents

Experimental Section.....	2
X-ray crystal structures.....	4
DFT calculations.....	8
NMR spectral data.....	9
NMR spectra for [(1) ₂ Pd] (2).....	9
NMR spectra for [(1)Pd(μ-OH)] ₂ (3).....	11
NMR spectra for [Bu ₄ N][(1)Pd(CH ₃)Cl] (4).....	13
NMR spectra for [(1)Pd(CH ₃)(py)] (5).....	16
NMR spectra for [Bu ₄ N][(1)Pd(COCH ₃)Cl] (6).....	19
NMR spectra for [(1)Pd(C(CH ₃)=NC ₆ H ₄ OMe)(CNC ₆ H ₄ OMe)] (7).....	24
NMR spectra for [(1)Pd(COCH ₃)(py)] (8).....	26
NMR spectra for [(1)Pd(CH(Et)CO ₂ Me)(py)] (9).....	29
<i>In situ</i> NMR reactivity studies.....	32
Attempted chloride abstraction from 4.....	36
UV-Vis absorption spectra.....	43
Cyclic voltammetry data.....	44
Attempted catalytic reactions.....	45
References.....	47

Experimental Section

General Considerations. All manipulations were carried out under nitrogen or argon using standard glovebox, Schlenk, and vacuum-line techniques. For the synthesis of complex **2** and **3**, the solvents acetone, *n*-hexane and THF (Aldrich, anhydrous, 99.8 %) were used without further purification, while anhydrous dichloromethane was freshly distilled over CaH₂ under an argon atmosphere. For the synthesis of complex **4**, THF (Aldrich, anhydrous, 99.8%) was dried by percolation over columns of Al₂O₃ (Fluka); hexane (Aldrich, anhydrous, 99.8%) was passed over columns of Al₂O₃ (Fluka), BASF R3-11-supported Cu oxygen scavenger, and molecular sieves (Aldrich, 4 Å). NMR solvents were either used as received (CD₂Cl₂, Sigma-Aldrich), or vacuum transferred from Na/K alloy and stored under nitrogen (THF-*d*₈, Euriso-top). Compounds **1H**¹ and **1K**² were synthesized according to literature procedures. [Pd(CH₃)Cl(COD)] was either prepared according to the literature procedure,³ or obtained commercially (99%, Strem Chemicals). HCl (37%, Fluka) and 1,5-*cis,cis*-cyclooctadiene (Fluka) (used for the synthesis of [Pd(CH₃)Cl(COD)]), and tetrabutylammonium chloride (99%, Sigma-Aldrich), 4-methoxyphenyl isocyanide (97%, Sigma-Aldrich) and [Pd(CH₃COO)₂] (Engelhard Italy) were used as received. 1D and 2D NMR spectra were recorded on Varian Gemini 400, Mercury 400 or Inova 500 spectrometers. The resonances are reported in ppm (δ) and referenced to the residual solvent peak versus Si(CH₃)₄: CD₂Cl₂ at δ 5.32 (¹H) and δ 53.84 ppm (¹³C), THF-*d*₈ at δ 3.58 (¹H) and δ 67.21 ppm (¹³C). The assignment of NMR resonances was aided by gradient-selected COSY, NOESY, HSQC, and/or HMBC experiments using standard pulse sequences.

The infrared spectrum of compound **2** was recorded on a Perkin–Elmer FT-IR 2000 spectrometer in transmission mode and the sample was prepared as a KBr pellet. The infrared spectrum of compound **4** was recorded on a INTERSPEC FT-IR spectrometer in transmission mode under N₂ atmosphere and the sample was prepared by evaporation of a THF solution of the compound on KBr plates. Elemental analyses were performed at the Microanalytical Department of the University of Groningen. Cyclic voltammetry was performed using a three-electrode setup with a silver wire pseudoreference electrode and a platinum disk working electrode (CHI102, CH Instruments; diameter = 2 mm). The platinum working electrode was polished before the experiment using an alumina slurry (0.05 μm), rinsed with distilled water, and subjected to brief ultrasonication to remove any adhered alumina microparticles. The electrodes were then dried in an oven at 75 °C overnight to remove any residual traces of water. The CV data were calibrated by adding ferrocene or decamethylferrocene as a THF solution at the end of the experiments. There is no indication that the addition of ferrocene and or decamethylferrocene influences the electrochemical behavior of the products. All electrochemical measurements were performed at ambient temperatures under an inert N₂ atmosphere in THF containing 0.1 M [nBu₄N][PF₆] as the supporting electrolyte. Data were recorded with *Autolab NOVA* software (version 1.8 and version 2.0).

Synthesis of [Pd(1)₂] (2). [Pd(CH₃CO₂)₂] (1 eq, 100.0 mg, 0.45 mmol) was dissolved at room temperature in acetone (12 mL). After stirring for 30 min, the mixture was filtered on paper obtaining a brownish-red clear solution. The ligand **1H** (2 eq, 283.0 mg, 0.9 mmol) was added as a solid to the solution, which immediately became intensely red colored. The reaction mixture was stirred for 5 h at room temperature, observing a change of color towards darker tonality. After concentration of the mixture and storage at +4 °C overnight, a dark solid precipitated and it was filtered off and washed with cold acetone, affording 140.6 mg of product (0.19 mmol, 43 %). Single crystals suitable for X-ray diffraction were obtained by slow diffusion of *n*-hexane into a chloroform solution of **2** at 4 °C. ¹H NMR (500 MHz, CD₂Cl₂, 25 °C): δ 8.04 (d, 4H, *p*-tolyl *o*-CH), 7.63 (d, 8H, Ph *o*-CH), 7.35 (d, 4H, *p*-tolyl *m*-CH), 7.10 (t, 8H, Ph *m*-CH), 7.01 (m, 4H, Ph *p*-CH), 2.47 (s, 3H, *p*-tolyl CH₃) ppm. ¹H-¹³C HSQC NMR (500 MHz, CD₂Cl₂, 25 °C) δ 129.04 (*p*-tolyl *m*-C), 128.06 (Ph *m*-C), 126.56 (Ph *p*-C), 124.61 (*p*-tolyl *o*-C), 123.21 (Ph *o*-C), 20.87 (*p*-tolyl CH₃). Anal. calcd for C₄₀H₃₄N₈Pd: C 65.53, H 4.67, N 15.28; found: C 65.46, H 4.70, N 15.14. IR: ν_{max} = 1269 (stretch C-N), 1198 (stretch N-N) cm⁻¹. MS (ESI, CH₃Cl): *m/z* = 755.2 [M + Na⁺], 732.2 [M + H⁺].

Reaction of [Pd(COD)(CH₃)Cl] with 1K: formation of [(1)Pd(μ-OH)]₂ (3). [Pd(COD)(CH₃)Cl] (50.0 mg, 1 eq, 0.19 mmol) was dissolved in a Schlenk flask, under inert atmosphere, in THF (7 mL) leading to a pale yellow solution. **1K** (94.5 mg, 0.5 eq, 0.095 mmol) was added to the solution leading to a violet reaction mixture that was stirred at room temperature for 30 min, observing that its color turned blue. After concentration and precipitation with *n*-hexane at +4 °C, a blue solid was obtained. The ¹H NMR spectrum showed the presence of two major species, **2** and **3** (in ratio 4:1 respectively).

Repeating the same reaction at 0 °C led to a mixture in which **3** was present as the major species based on ¹H NMR spectroscopy (**2:3** ratio = 0.25:1). From this crude material, we were able to obtain **3** in crystalline form by slow diffusion of *n*-hexane into an NMR solution in CD₂Cl₂ at 4 °C. NMR data for **3**: ¹H NMR (500 MHz, CD₂Cl₂, 25 °C): δ 7.78 (d, 4H, *p*-tolyl *o*-CH), 7.68 (d, 8H, Ph *o*-CH), 7.24-7.14 (m, 16 H Ph *m*-CH; Ph *p*-CH; *p*-tolyl *m*-CH), 2.36 (s, 6H, *p*-tolyl CH₃), -3.46 (s, 2H, μ-OH). ¹H-¹³C HSQC NMR (500 MHz, CD₂Cl₂, 25 °C) δ = 129.16, (*p*-tolyl *m*-C), 128.94 (Ph *m*-C), 127.85 (Ph *p*-C), 124.66 (*p*-tolyl *o*-C), 123.94 (Ph *o*-C), 20.98 (*p*-tolyl CH₃).

X-ray crystal structures

X-ray crystallography. Single crystal data of **2** and **3** were collected at the X-ray diffraction beamline XRD1 of the ELETTRA Synchrotron, Trieste (Italy), using the rotating crystal method with a monochromatic wavelength of 0.7000 Å, on a Dectris Pilatus 2M detector. Measurements were performed at 100(2) K using a nitrogen stream cryo-cooler. Cell refinement, indexing and scaling of the data sets were performed using the CCP4 package,⁴ and programs Denzo and Scalepack.⁵ The structures were solved by direct methods and Fourier analyses and refined by the full-matrix least-squares method based on F^2 with all observed reflections.⁶ All non-hydrogen atoms were refined with anisotropic displacement coefficients. For compound **4**, a single crystal was mounted on top of a cryoloop and transferred into the cold nitrogen stream (100 K) of a Bruker-AXS D8 Venture diffractometer. Data collection and reduction was done using the Bruker software suite APEX3.⁷ The final unit cell was obtained from the xyz centroids of 9783 reflections after integration. A multiscan absorption correction was applied, based on the intensities of symmetry-related reflections measured at different angular settings (SADABS). The structures were solved by direct methods using SHELXT⁸ and refinement of the structure was performed using SHELXL.⁹ Refinement was frustrated by a disorder problem: the last two C atoms of one of the butyl groups in the Bu₄N cation showed unrealistically large anisotropic displacement parameters. A two-site occupancy model was applied, which refined to a s.o.f. of 0.66 for the major fraction. The hydrogen atoms were generated by geometrical considerations, constrained to idealised geometries and allowed to ride on their carrier atoms with an isotropic displacement parameter related to the equivalent displacement parameter of their carrier atoms. Crystal data and details on data collection and refinement are presented in Table S1.

Table S1. Crystallographic data for **2**, **3** and **4**.

	2	3	4
chem formula	C ₄₀ H ₃₄ N ₈ Pd·CHCl ₃	C ₄₀ H ₃₆ N ₈ O ₂ Pd ₂ ·CH ₂ Cl ₂	C ₃₇ H ₅₆ N ₅ ClPd
M _r	852.52	958.49	712.71
cryst syst	triclinic	triclinic	monoclinic
color, habit	dark brown, needle	blue, block	blue, block
space group	P -1	P -1	P 21/n
a (Å)	8.0390(16)	9.897(2)	14.8027(6)
b (Å)	8.1400(16)	12.993(3)	16.6849(6)
c (Å)	14.734(3)	16.703(3)	15.6639(6)
α (°)	98.99(3)	105.23(3)	90
β (°)	90.96(3)	106.50(3)	107.675(2)

γ (°)	99.37(3)	98.54(3)	90
V (Å ³)	938.7(3)	1928.5(8)	3686.1(2)
Z	1	2	4
ρ_{calc} , g.cm ⁻³	1.508	1.651	1.284
Radiation [Å]	Mo K α 0.700	Mo K α 0.700	Mo K α 0.71073
μ (Mo K α), mm ⁻¹	0.750	1.119	0.607
F(000)	434	964	1504
Temp (K)	100(2)	100(2)	100(2)
θ range (°)	1.38-30.00	1.65-29.54	2.89 – 27.17
data collected (h,k,l)	-11:11; -11:11; -21:21	-13:12; -18:18; -23:23	-18:19; -21:21; -20:19
no. of reflns collected	34320	58674	54583
no. of indepndt reflns	5604	11162	8160
Observed reflns	5600	10833	6732
$F_o \geq 2.0 \sigma (F_o)$			
R(F) (%)	2.77	3.68	5.70
wR(F ²) (%)	7.71	10.35	11.99
GooF	1.198	1.059	1.197
weighting a,b	0.0399, 0.6900	0.0526, 5.2674	0.0049, 16.4500
params refined	260	505	423
min, max resid dens	-1.296, 1.250	-2.442, 2.770	-0.922, 2.203

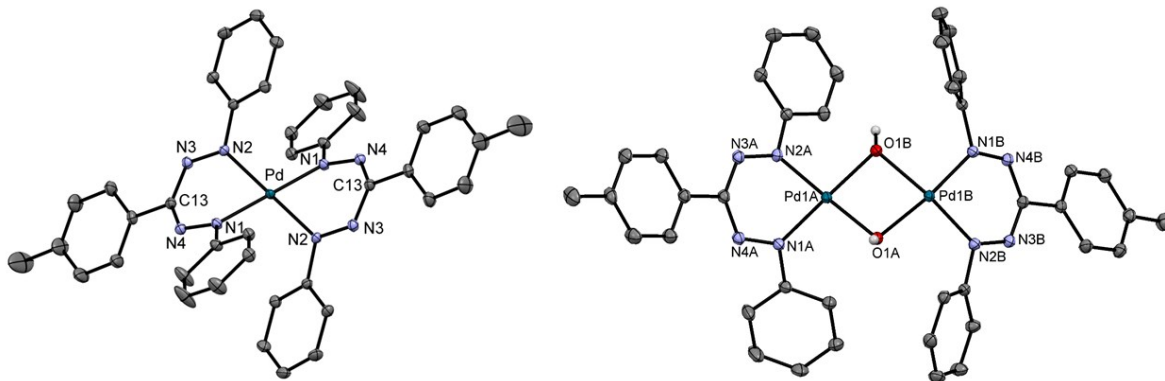


Figure S1. ORTEP drawing (ellipsoids at 50% probability) of compounds **2** (left) and **3** (right) with atom labeling scheme of the non-C atoms. Hydrogen atoms (except for the OH groups in **3**) are omitted for clarity.

Table S2. Selected bond lengths (Å) and angles (°) in compounds **2**, **3** and **4**.

	2	3	4
	(x = none)	(x = A)	(x = B)
Pd(1x)-N(1x)	2.0265(13)	1.992(2)	1.963(2)
Pd(1x)-N(2x)	2.0162(13)	1.991(2)	1.975(2)
Pd(1x)-O(1A)		2.0317(18)	2.0428(18)
Pd(1x)-O(1B)		2.0567(18)	2.0781(18)
Pd(1)-Cl(1)			
Pd(1)-C(21)			2.3055(10)
N(1x)-N(4x)	1.2956(16)	1.291(3)	1.285(3)
N(2x)-N(3x)	1.2925(15)	1.291(3)	1.289(3)
N(3x)-C(13x)	1.3507(18)	1.343(3)	1.345(3)
N(4x)-C(13x)	1.3426(18)	1.356(3)	1.350(3)
N(1x)-Pd(1x)-N(2x)	82.04(6)	82.92(9)	88.87(9)
$\angle(\text{N-Pd-N})/(\text{X-Pd-X})^a$	0.00	5.09	7.83

^a Dihedral angle between the coordination planes defined by the N-Pd-N and X-Pd-X atoms.

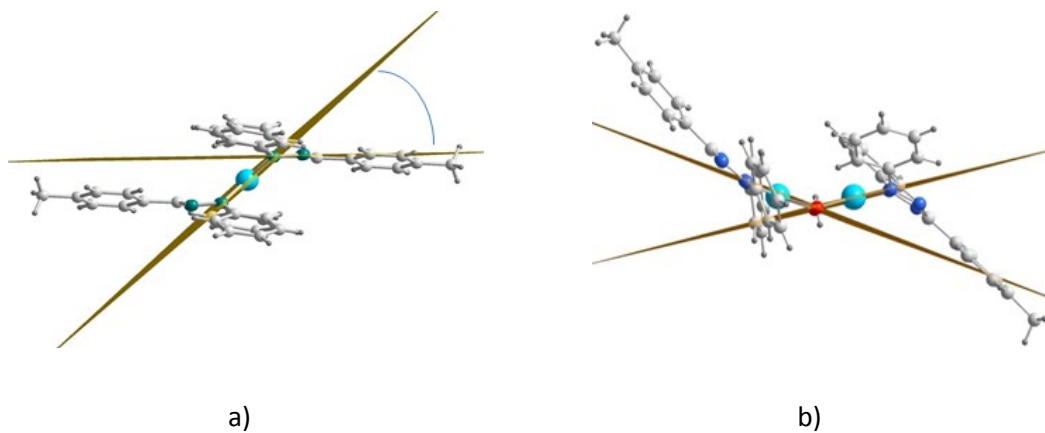


Figure S2. Side view of complexes: a) **2**, highlighting the dihedral angle between the square plane around the Pd center and the NNCNN backbone of the ligand; b) **3**, highlighting the 'fold' angle between the two O-Pd-O planes.

DFT calculations

Computational studies used the Gaussian09 software package.¹⁰ Geometry optimizations were carried out for the bis(formazanate) palladium compound $[(\mathbf{1})_2\text{Pd}]$ using DFT calculations with B3LYP functional and a 6-31+G(d,p) basis set for all atoms except Pd, for which a LANL2DZ basis set (with ECP) was used. Optimized geometries were verified to be minima on the potential energy surface by frequency calculations. Starting from the geometry of $[(\mathbf{1})_2\text{Pd}]$, also the geometries of the 1-electron reduced compound $[(\mathbf{1})_2\text{Pd}]^-$ and the 1-electron oxidized compound $[(\mathbf{1})_2\text{Pd}]^+$ were optimized (as doublet states using unrestricted DFT). Visualization of the molecular orbitals and spin density distributions was performed using Chemcraft 1.7 or Gaussview 5.0.

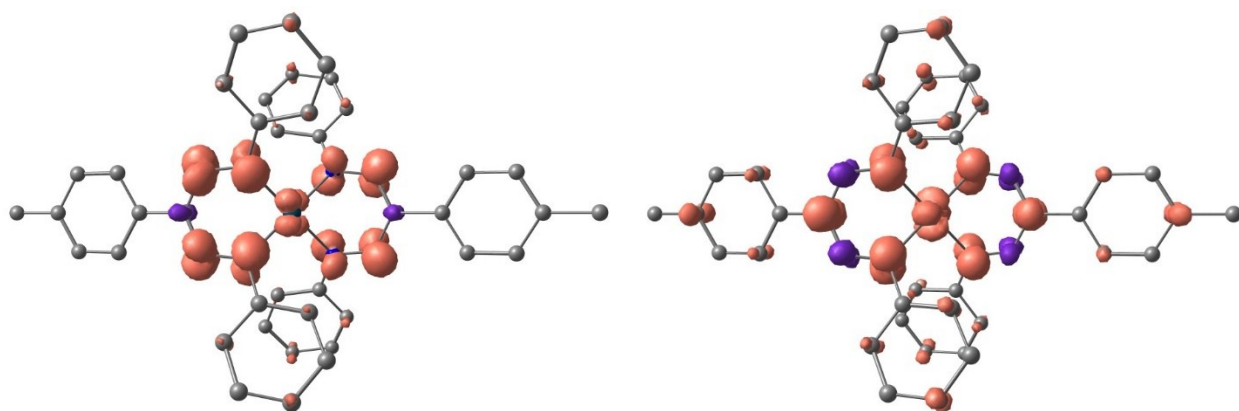


Figure S3. Spin density plot for the anion $[(\mathbf{1})_2\text{Pd}]^-$ (left) and the cation $[(\mathbf{1})_2\text{Pd}]^+$ (right, DFT optimized geometries).

NMR spectral data

NMR spectra for $[(1)_2\text{Pd}]$ (**2**)

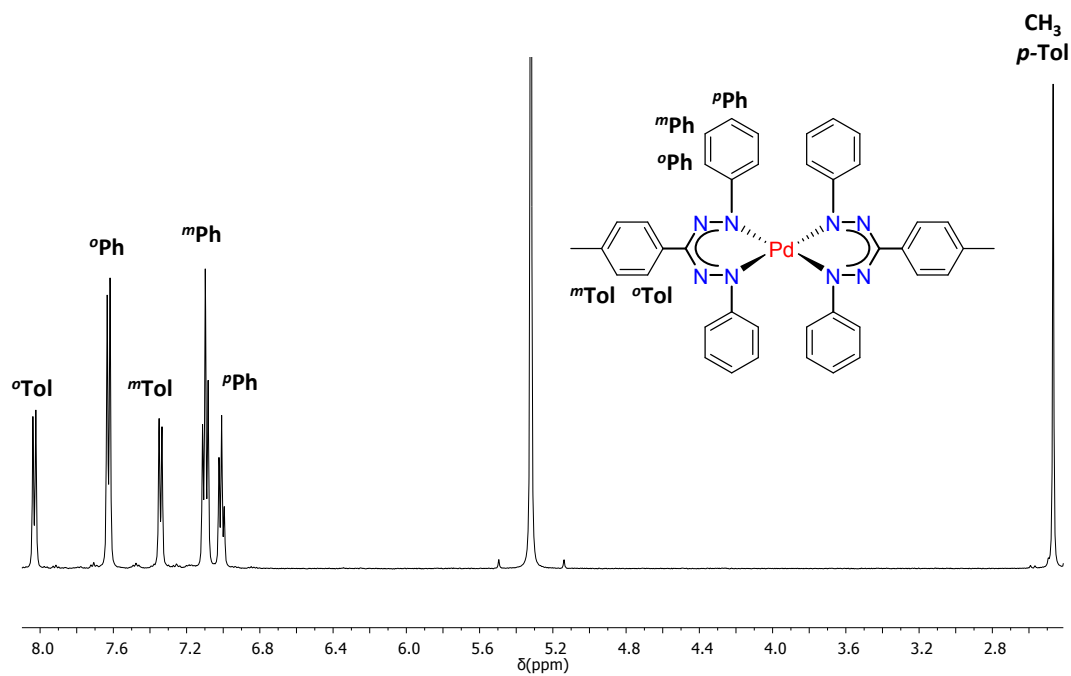


Figure S4. ^1H NMR spectrum of **2** (CD_2Cl_2 , $25\text{ }^\circ\text{C}$, 500 MHz).

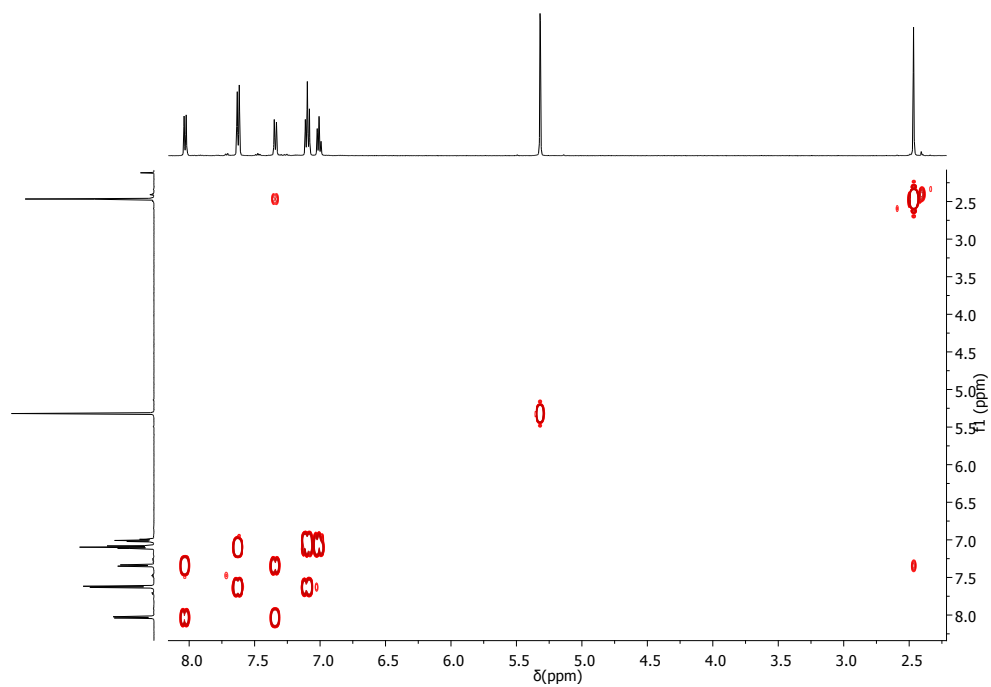


Figure S5. ^1H - ^1H COSY spectrum of **2**, (CD_2Cl_2 , $25\text{ }^\circ\text{C}$, 500 MHz).

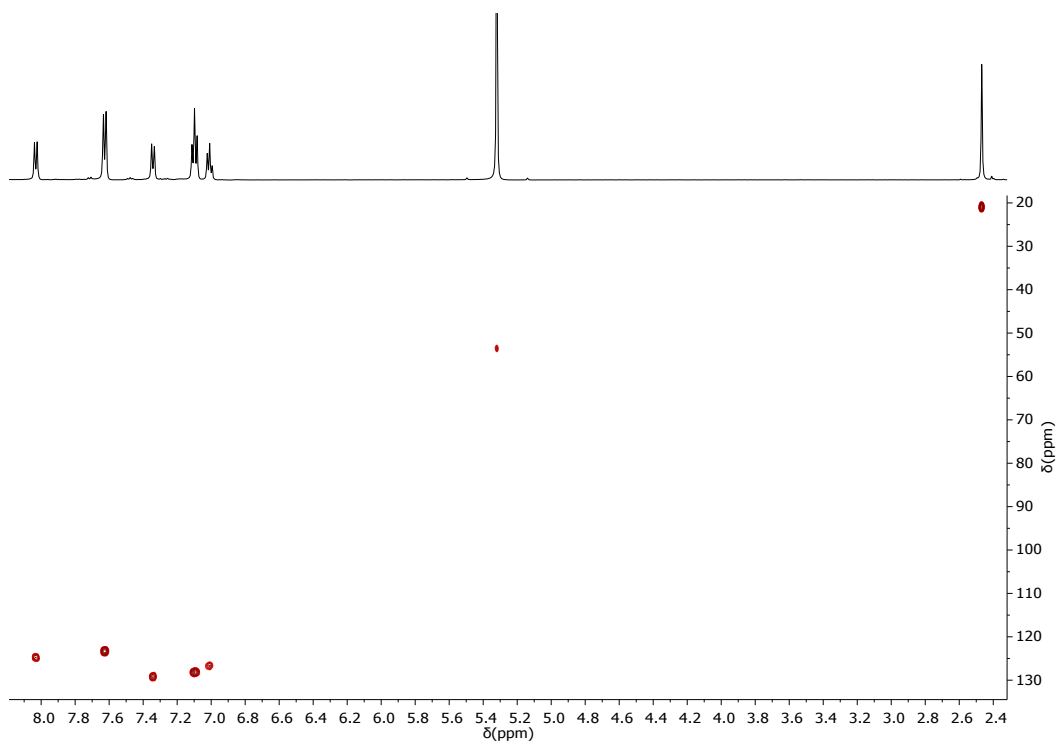


Figure S6. ^1H - ^{13}C HSQC spectrum of **2**, (CD_2Cl_2 , 25 °C, 500 MHz).

NMR spectra for $[(1)Pd(\mu-OH)]_2$ (3**)**

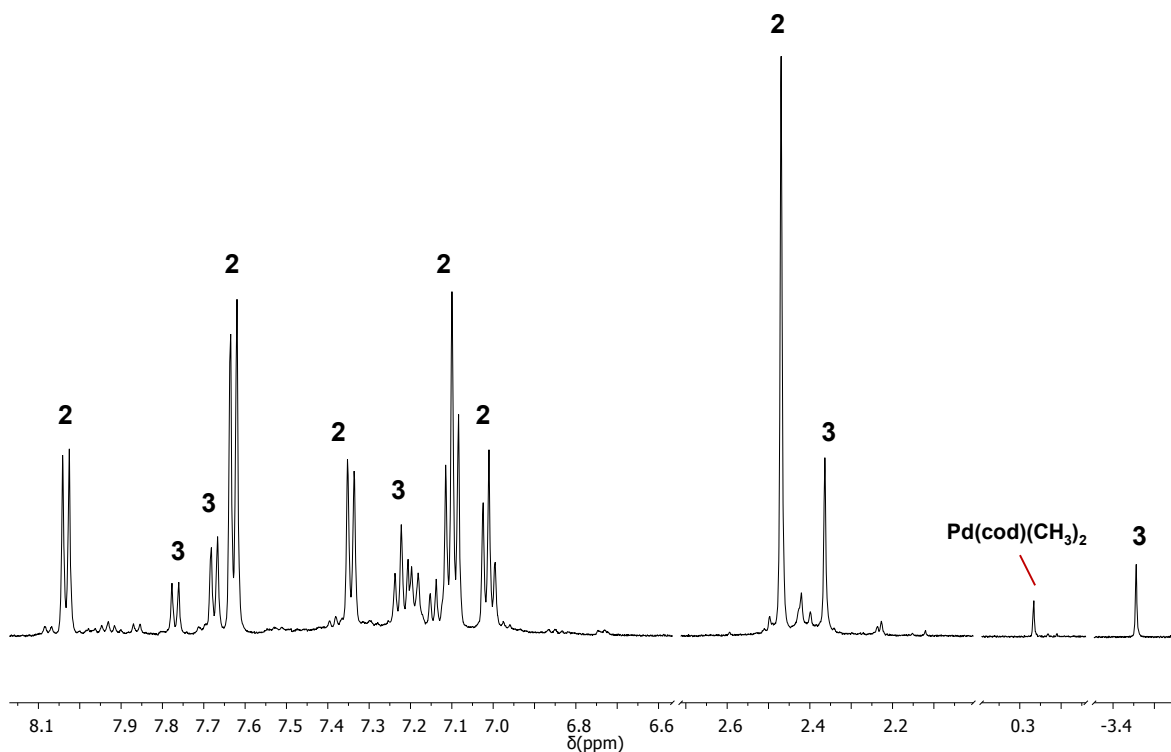


Figure S7. 1H NMR spectrum (CD_2Cl_2 , 25 °C, 500 MHz) of the solid isolated from the reaction of **1K** + $[Pd(COD)(CH_3)Cl]$ at room temperature, in THF. The aromatic and aliphatic regions are not on scale.

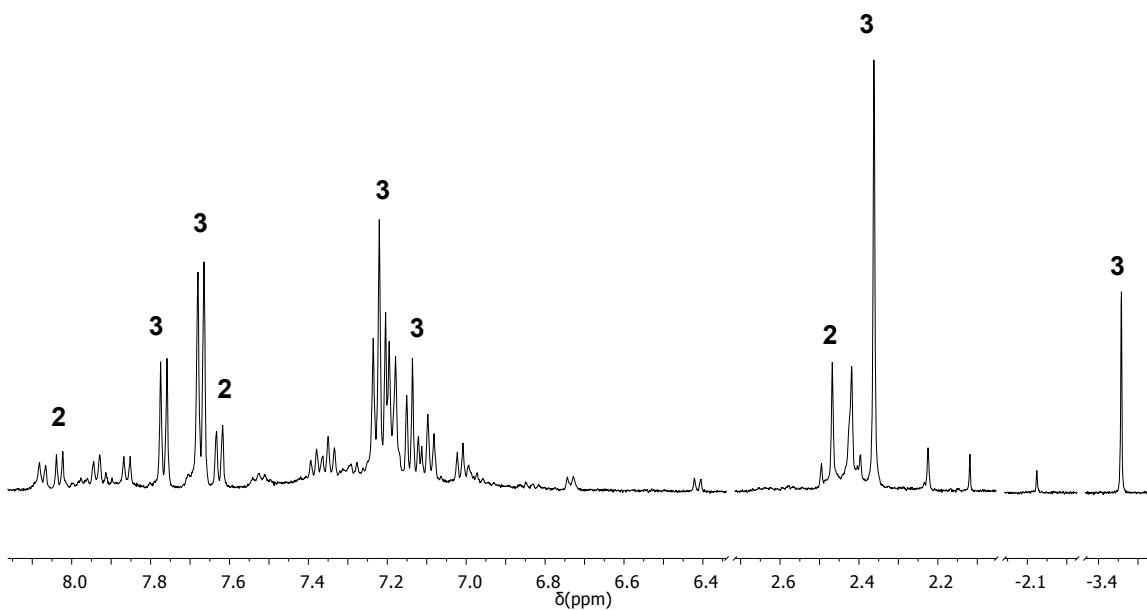


Figure S8. 1H NMR spectrum (CD_2Cl_2 , 25 °C, 500 MHz) of the isolated solid from the reaction of **1K** + $[Pd(COD)(CH_3)Cl]$ at 0 °C in THF. The aromatic and aliphatic regions are not on scale.

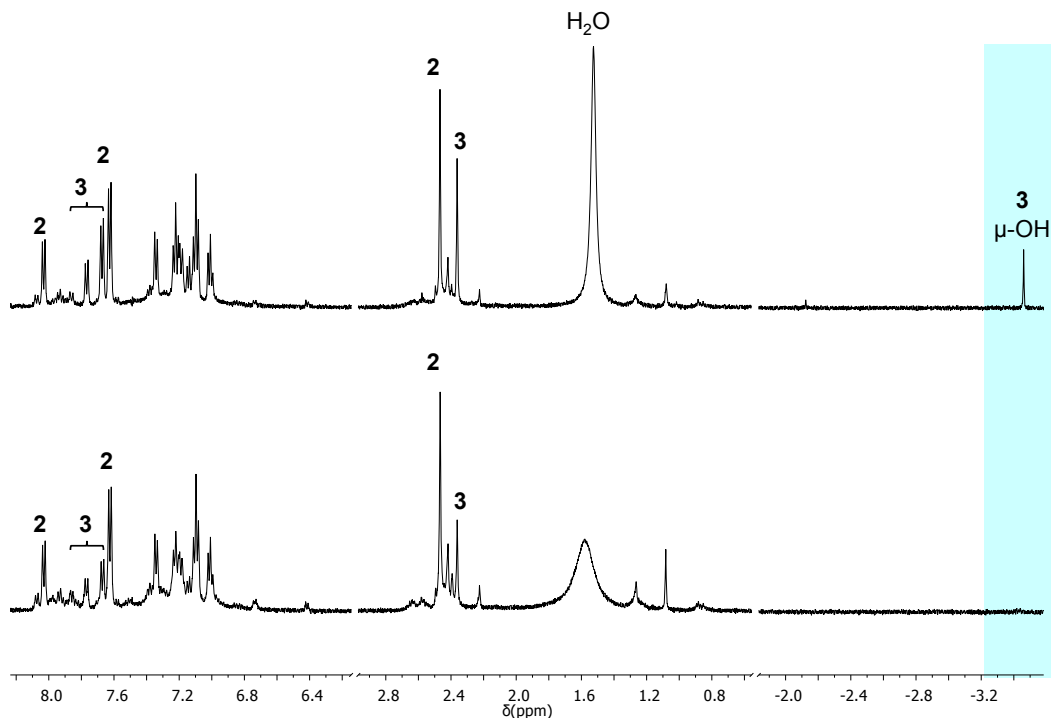


Figure S9. ^1H NMR (CD_2Cl_2 , 25 $^\circ\text{C}$, 500 MHz) of a) the solid isolated from the reaction of **1K** + $[\text{Pd}(\text{COD})(\text{CH}_3)\text{Cl}]$ at room temperature in THF, b) after addition of 2 μL of D_2O . The aromatic and aliphatic regions are not on scale.

NMR spectra for $[\text{Bu}_4\text{N}][(\text{1})\text{Pd}(\text{CH}_3)\text{Cl}]$ (4**)**

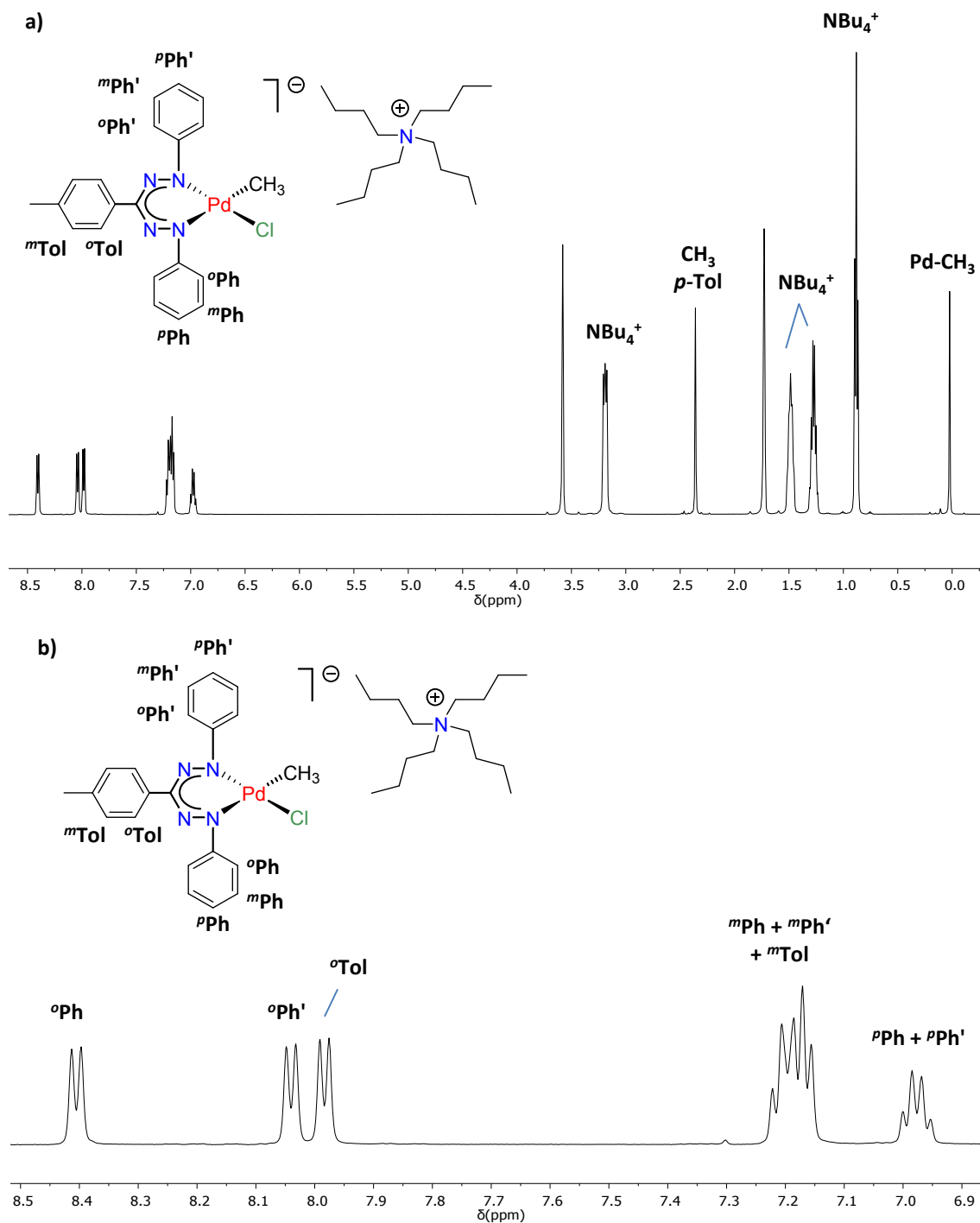


Figure S10. ^1H NMR spectrum of **4** ($\text{THF-}d_8$, 25°C , 500 MHz): a) full spectrum, b) aromatic region.

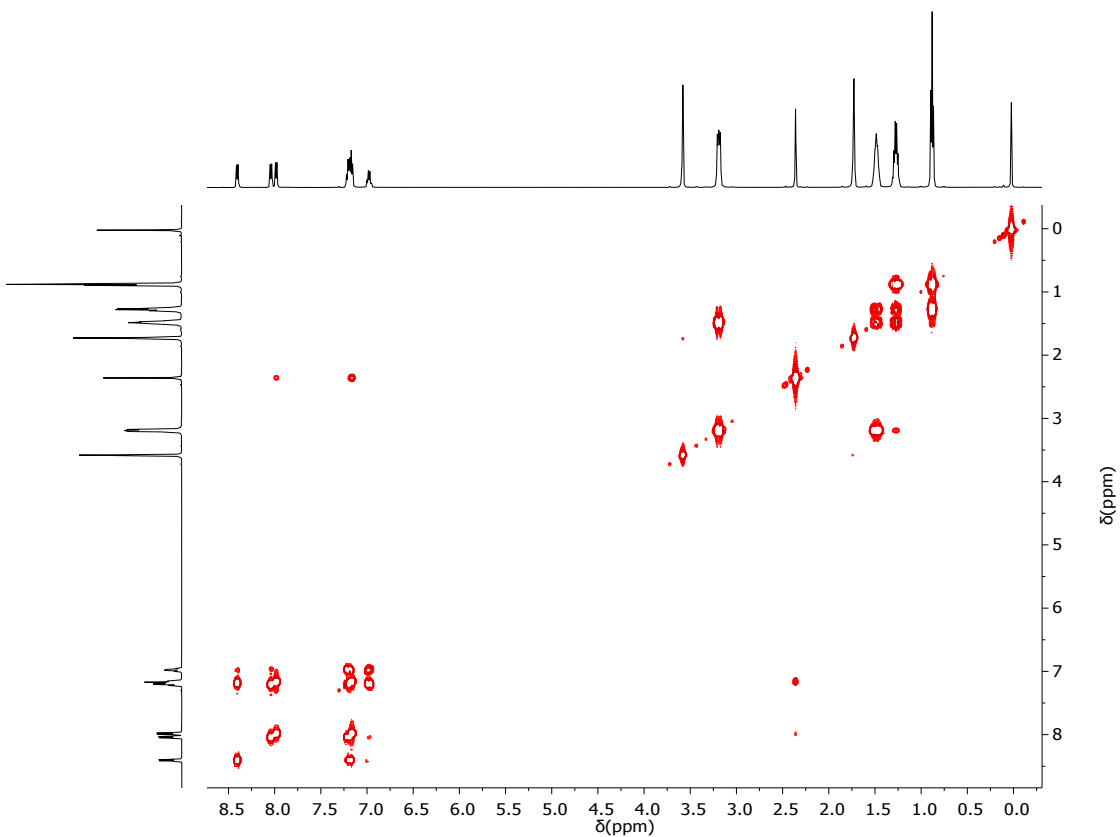


Figure S11. ^1H - ^1H COSY spectrum of **4**, ($\text{THF-}d_8$, 25 °C, 500 MHz).

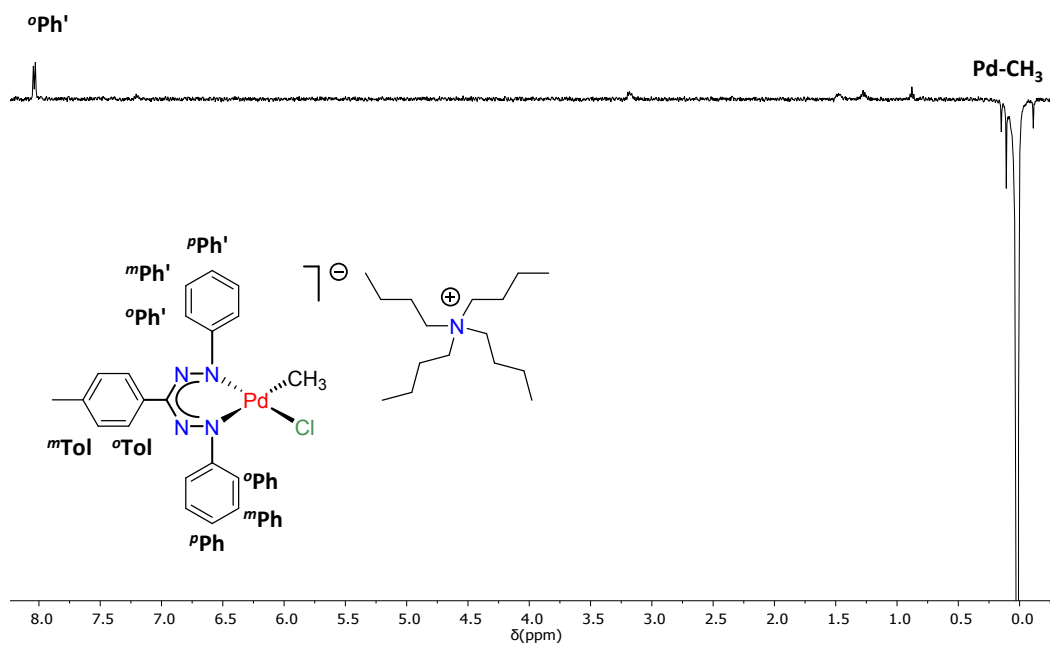


Figure S12. 1D NOESY spectrum of **4** ($\text{THF-}d_8$, 25 °C, 500 MHz), obtained by irradiating the signal at 0.02 ppm.

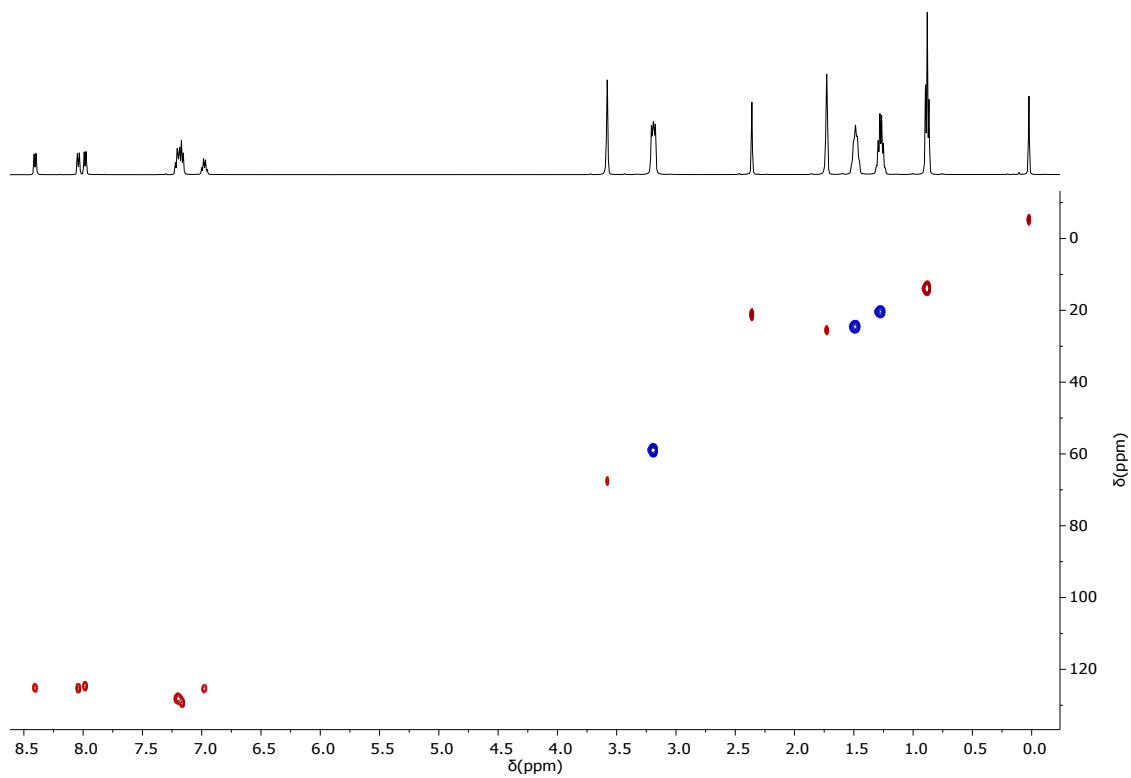


Figure S13. ^1H - ^{13}C HSQC spectrum of **4**, (THF- d_8 , 25 °C, 500 MHz).

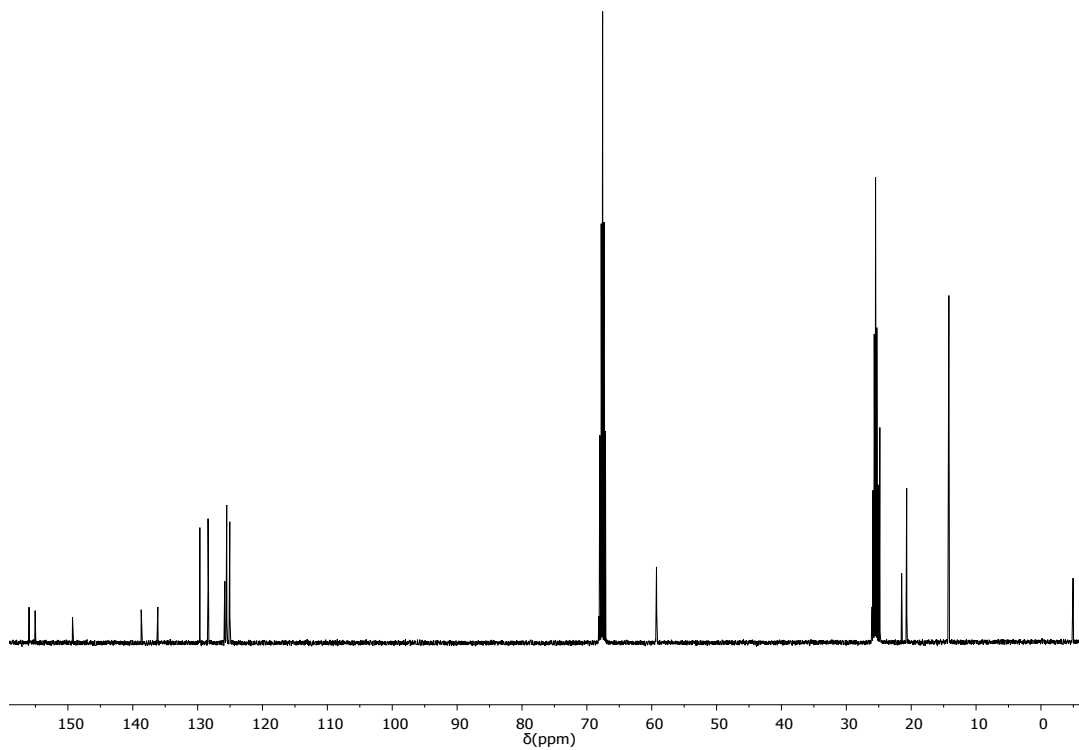


Figure S14. ^{13}C NMR spectrum of **4** (THF- d_8 , 25 °C, 101 MHz).

NMR spectra for [(1)Pd(CH₃)(py)] (5)

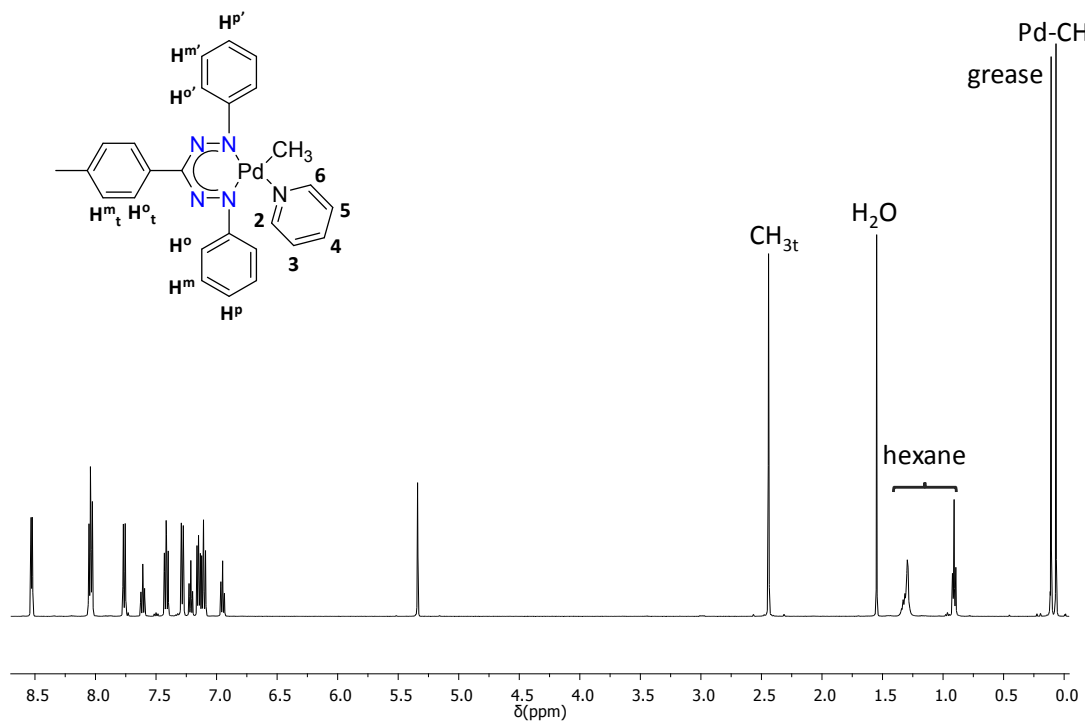


Figure S15. ¹H NMR spectrum of 5 (500 MHz, CD₂Cl₂, 25 °C).

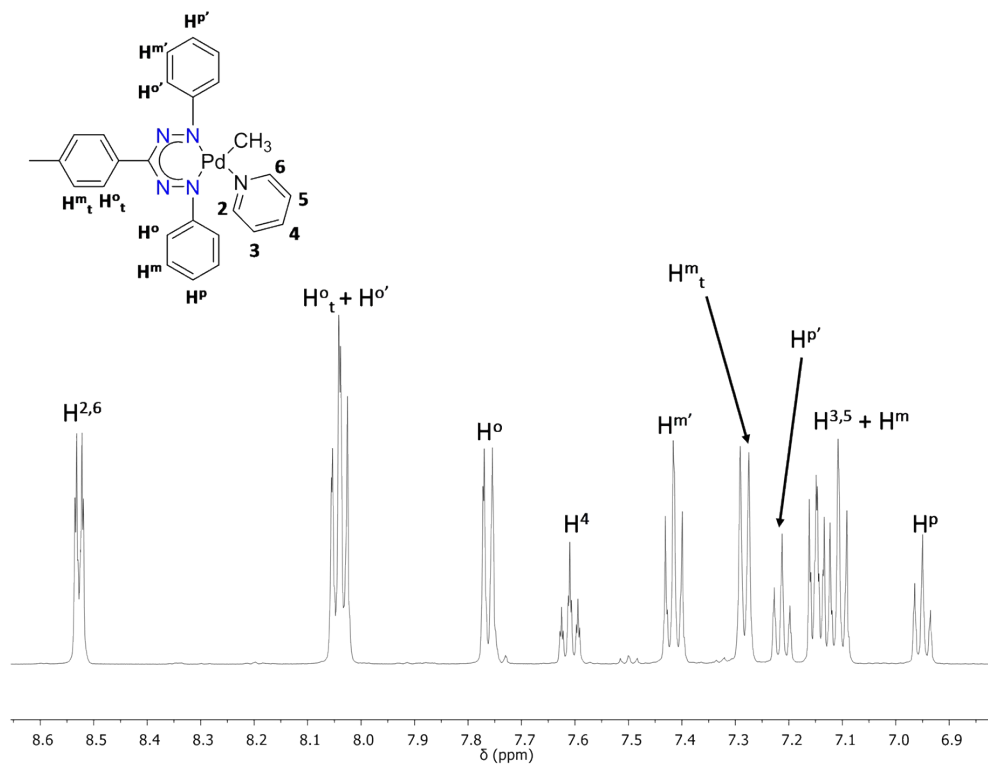


Figure S16. Enlargement of aromatic region of ¹H NMR spectrum of 5 (500 MHz, CD₂Cl₂, 25 °C).

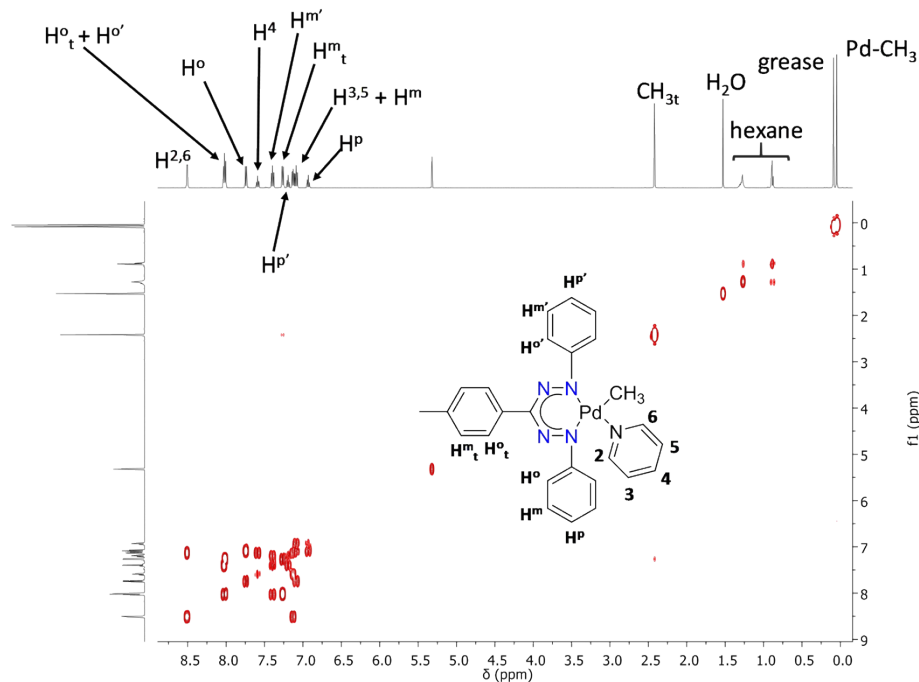


Figure S17. ^1H - ^1H COSY spectrum of **5** (400 MHz, CD_2Cl_2 , 25 °C).

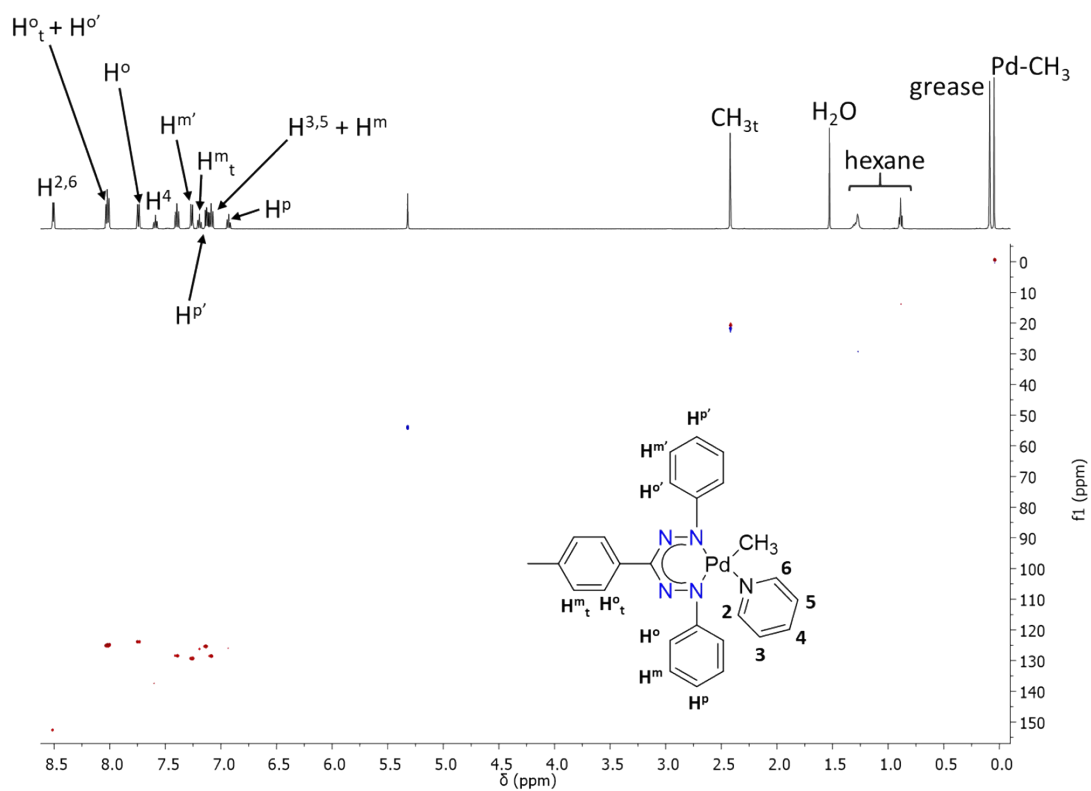


Figure S18. ^1H - ^{13}C HSQC spectrum of **5** (500 MHz, CD_2Cl_2 , 25 °C).

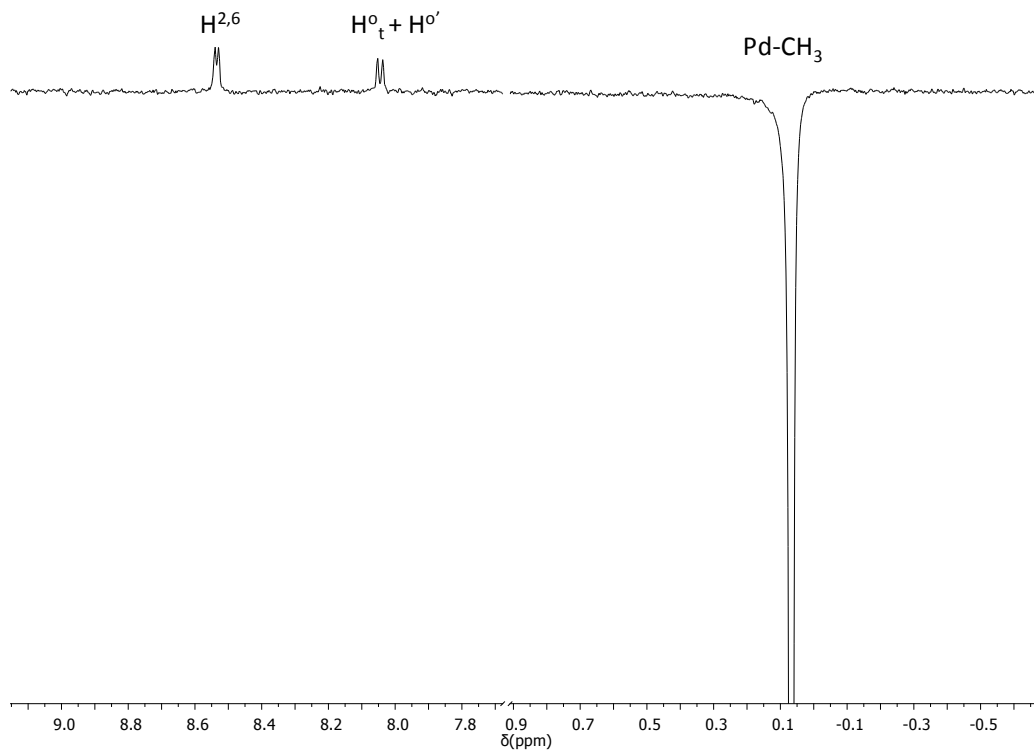


Figure S19. 1D NOESY spectrum of **5** (500 MHz, CD_2Cl_2 , 25 °C), obtained by irradiating the signal at 0.05 ppm.

NMR spectra for $[\text{Bu}_4\text{N}][(\text{1})\text{Pd}(\text{COCH}_3)\text{Cl}]$ (6**)**

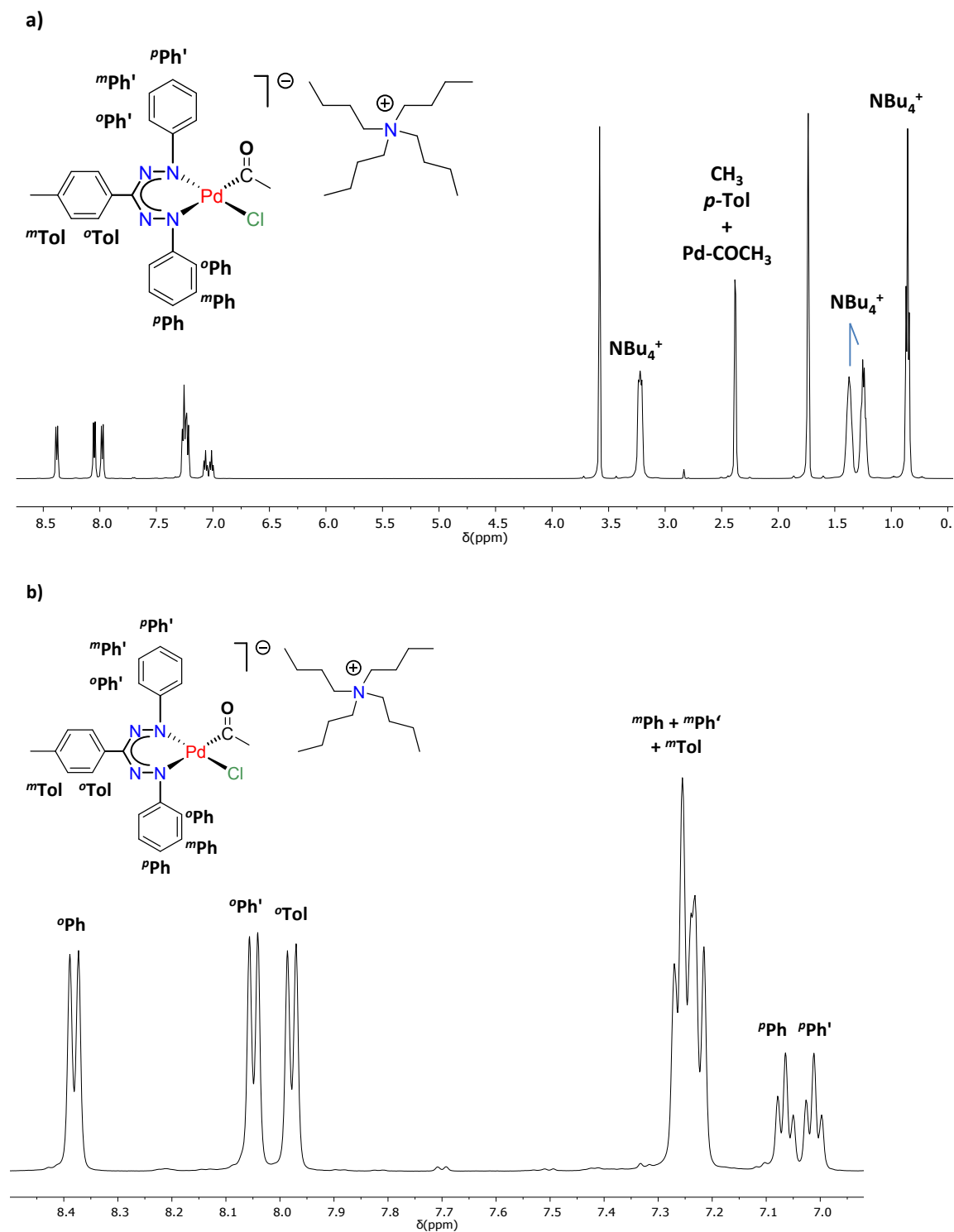


Figure S20. ^1H NMR spectrum of **6** from *in situ* NMR of **4** + CO (THF- d_8 , -40°C , 500 MHz): a) full spectrum, b) aromatic region.

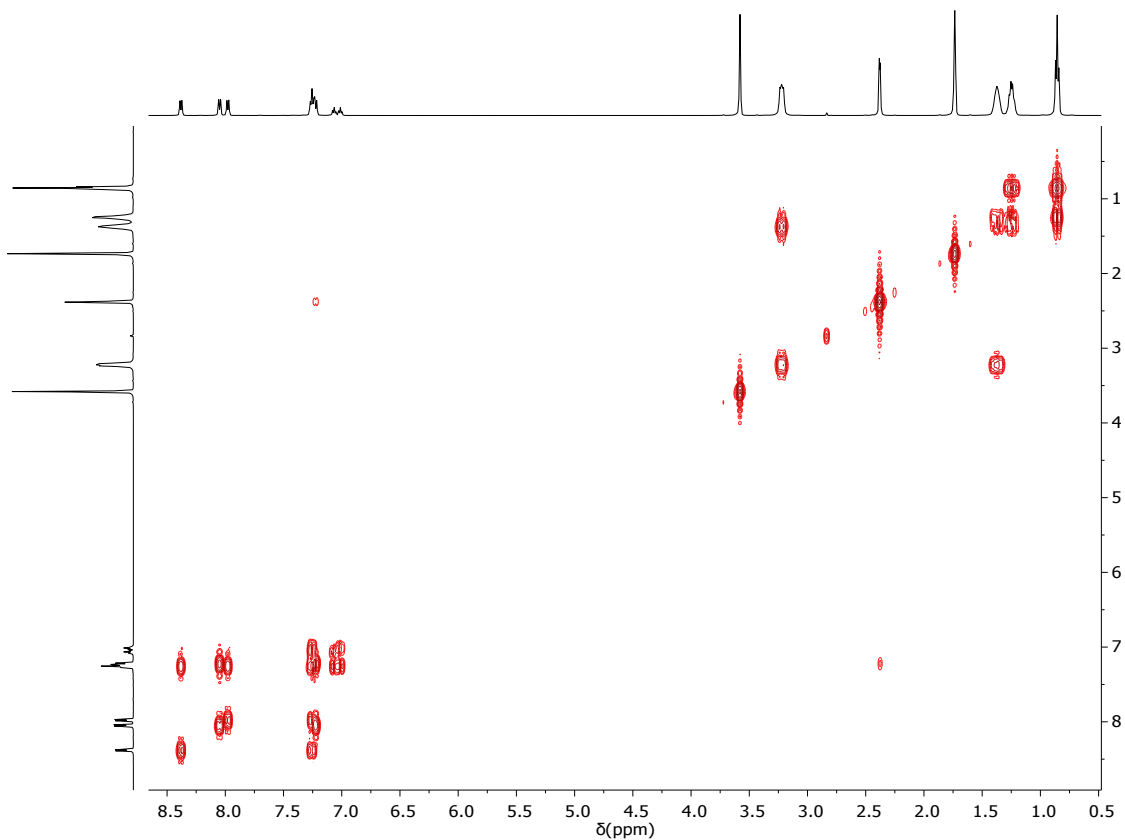


Figure S21. ^1H - ^1H COSY spectrum of **6** from *in situ* NMR of **4** + CO (THF- d_8 , -40 °C, 500 MHz).

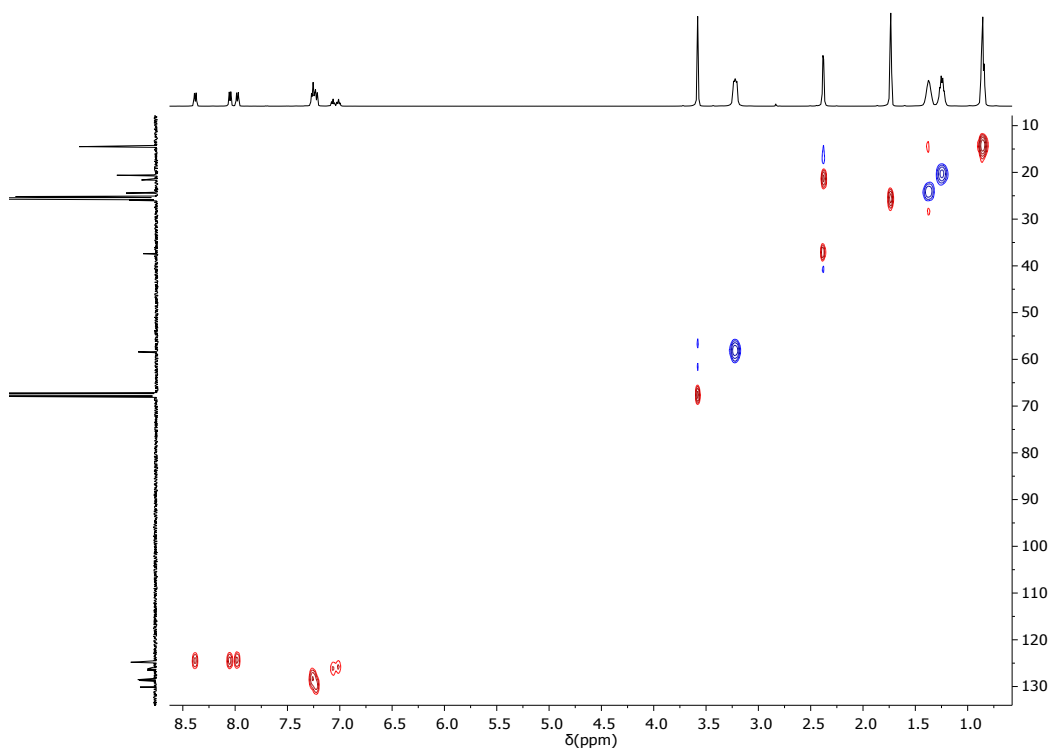


Figure S22. ^1H - ^{13}C gHSQCAD spectrum of **6** from *in situ* NMR of **4** + CO (THF- d_8 , -40 °C, 500 MHz).

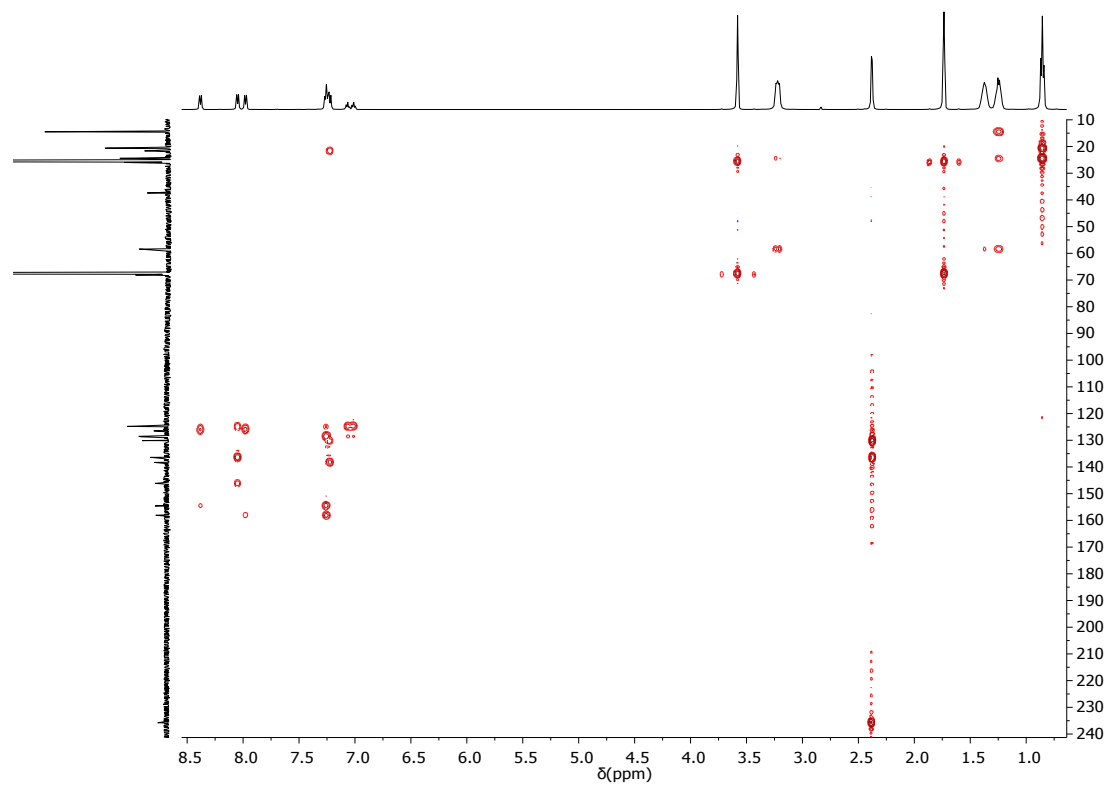


Figure S23. ^1H - ^{13}C gHMBCAD spectrum of **6** from *in situ* NMR of **4** + CO (THF- d_8 , -40 °C, 500 MHz).

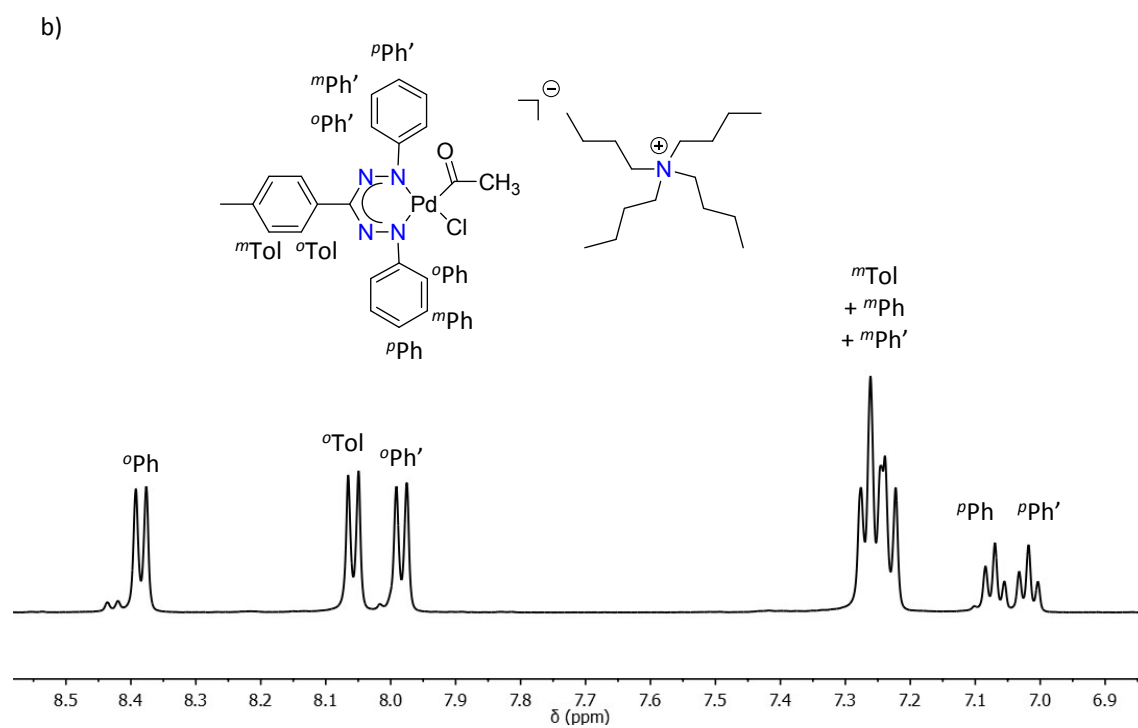
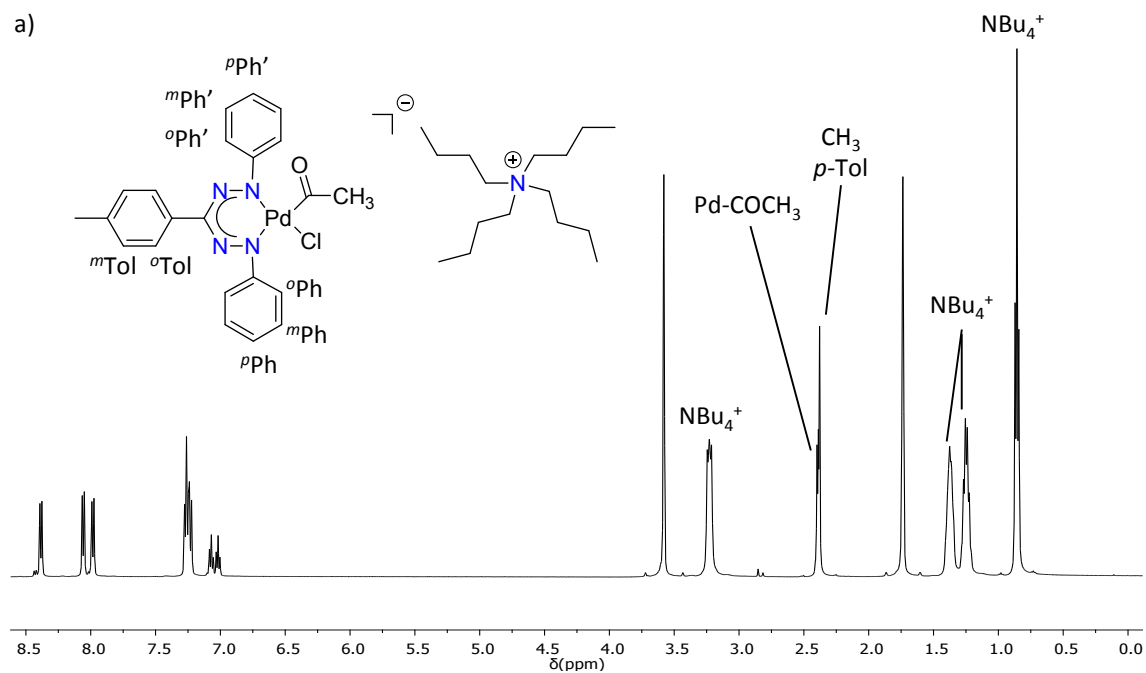


Figure S24. ^1H NMR spectrum of **6** from *in situ* NMR of **4** with ^{13}C O (THF- d_8 , -40°C , 500 MHz): a) full spectrum, b) aromatic region.

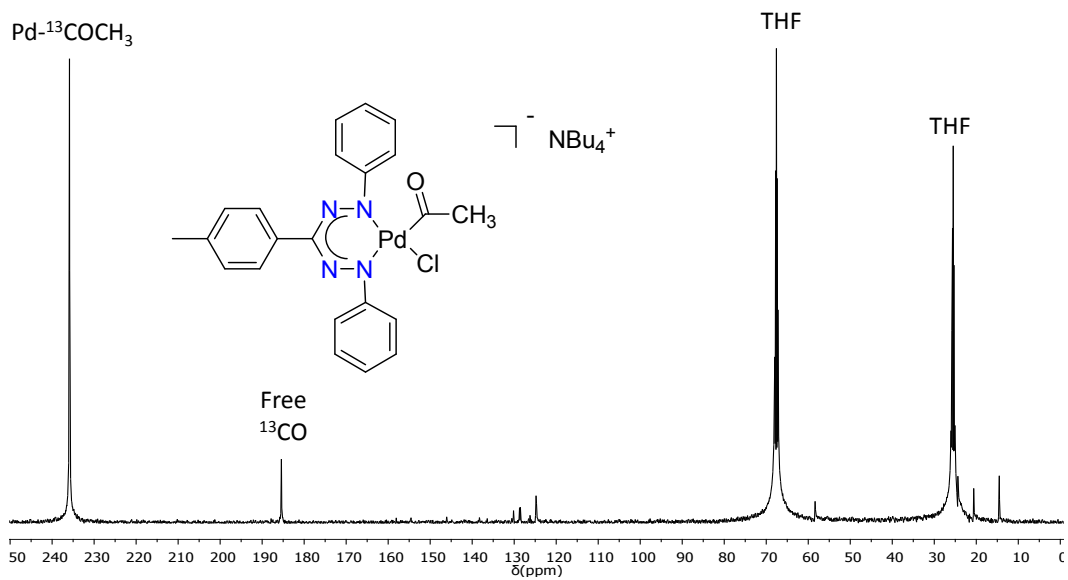


Figure S25. ^{13}C NMR spectrum of **6** from *in situ* NMR of **4** with ^{13}CO ($\text{THF-}d_8$, -40°C , 126 MHz).

NMR spectra for [(1)Pd(C(CH₃)=NC₆H₄OMe)(CNC₆H₄OMe)] (7)

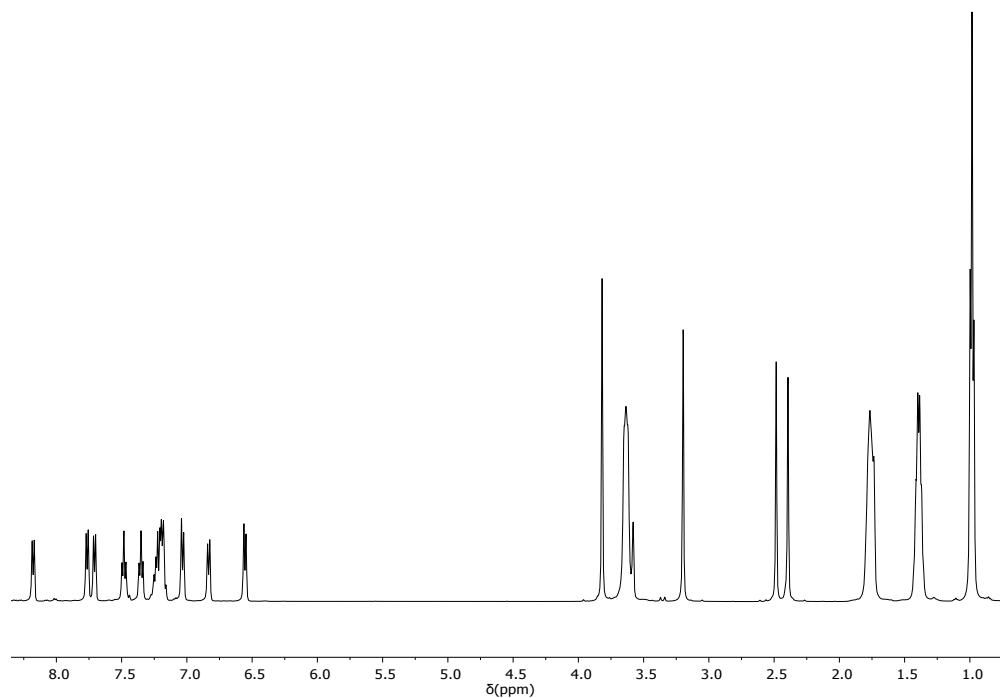


Figure S26. ¹H NMR spectrum of **7** from *in situ* NMR of **4** + 2 eq of CNC₆H₄OMe (THF-*d*₈, -40 °C, 500 MHz).

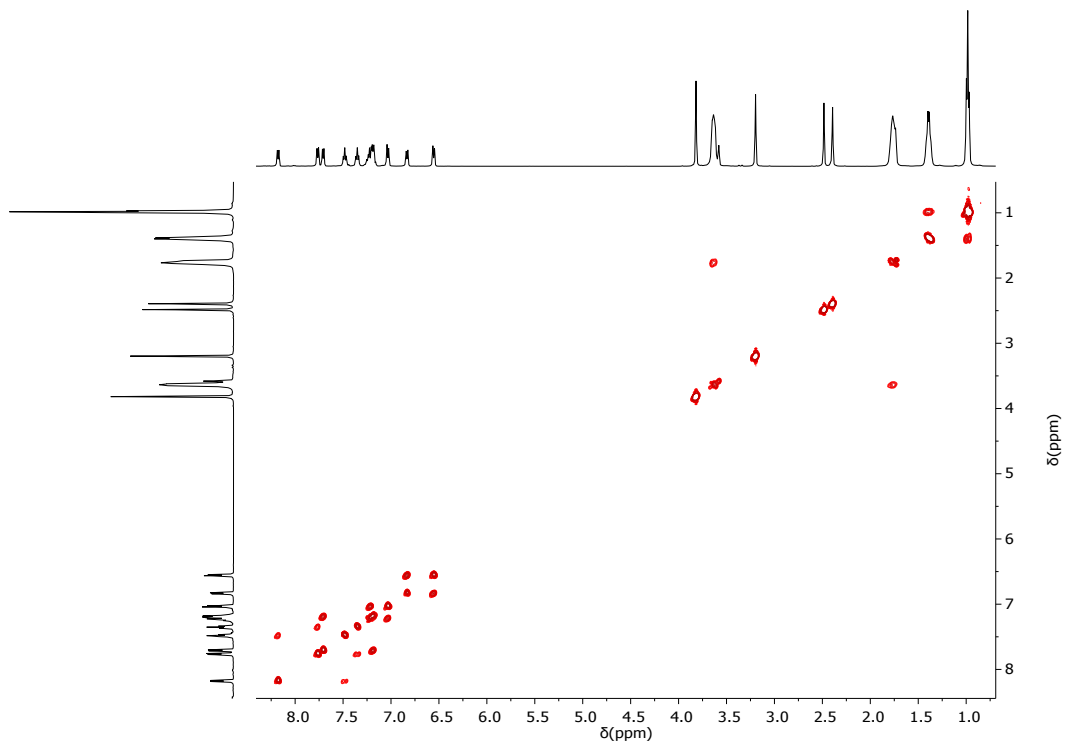


Figure S27. ¹H-¹H COSY spectrum of **7** from *in situ* NMR of **4** + 2 eq of CNC₆H₄OMe (THF-*d*₈, -40 °C, 500 MHz).

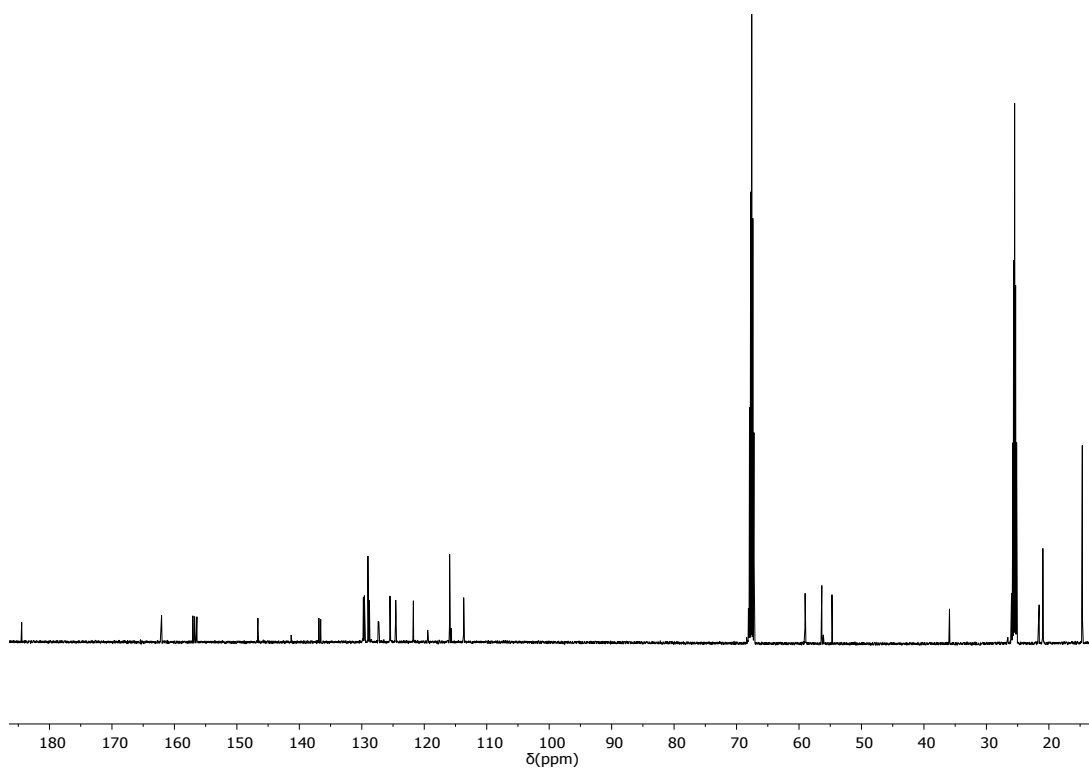


Figure S28. ^{13}C NMR spectrum of **7** from *in situ* NMR of **4** + 2 eq of $\text{CNC}_6\text{H}_4\text{OMe}$ ($\text{THF-}d_8$, $-40\text{ }^\circ\text{C}$, 126 MHz).

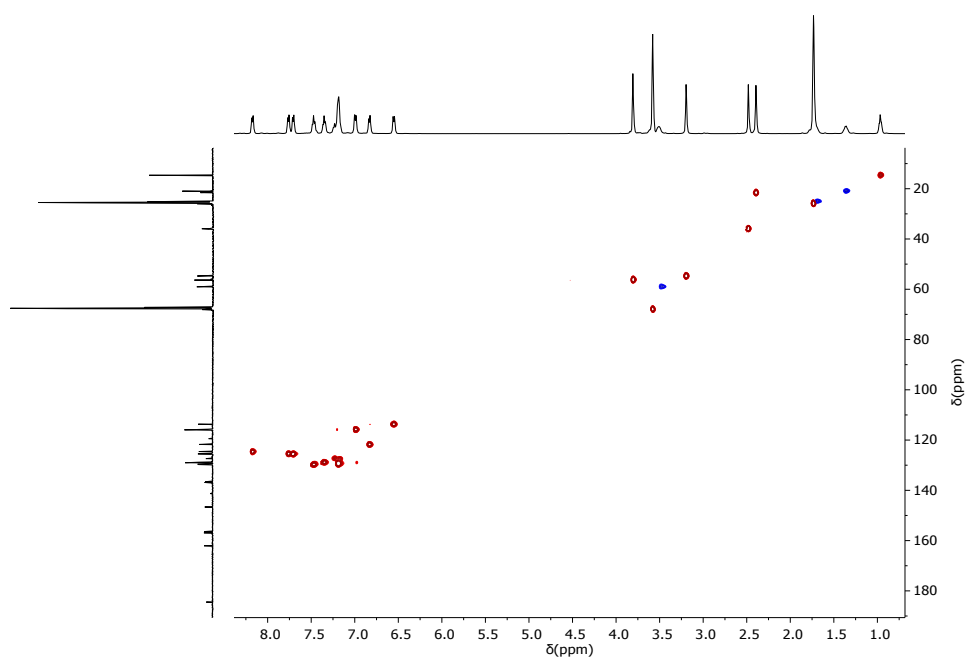


Figure S29. $^1\text{H-}^{13}\text{C}$ gHSQCAD spectrum of **7** from *in situ* NMR of **4** + 2 eq of $\text{CNC}_6\text{H}_4\text{OMe}$ ($\text{THF-}d_8$, $-40\text{ }^\circ\text{C}$, 500 MHz).

NMR spectra for [(1)Pd(COCH₃)(py)] (8)

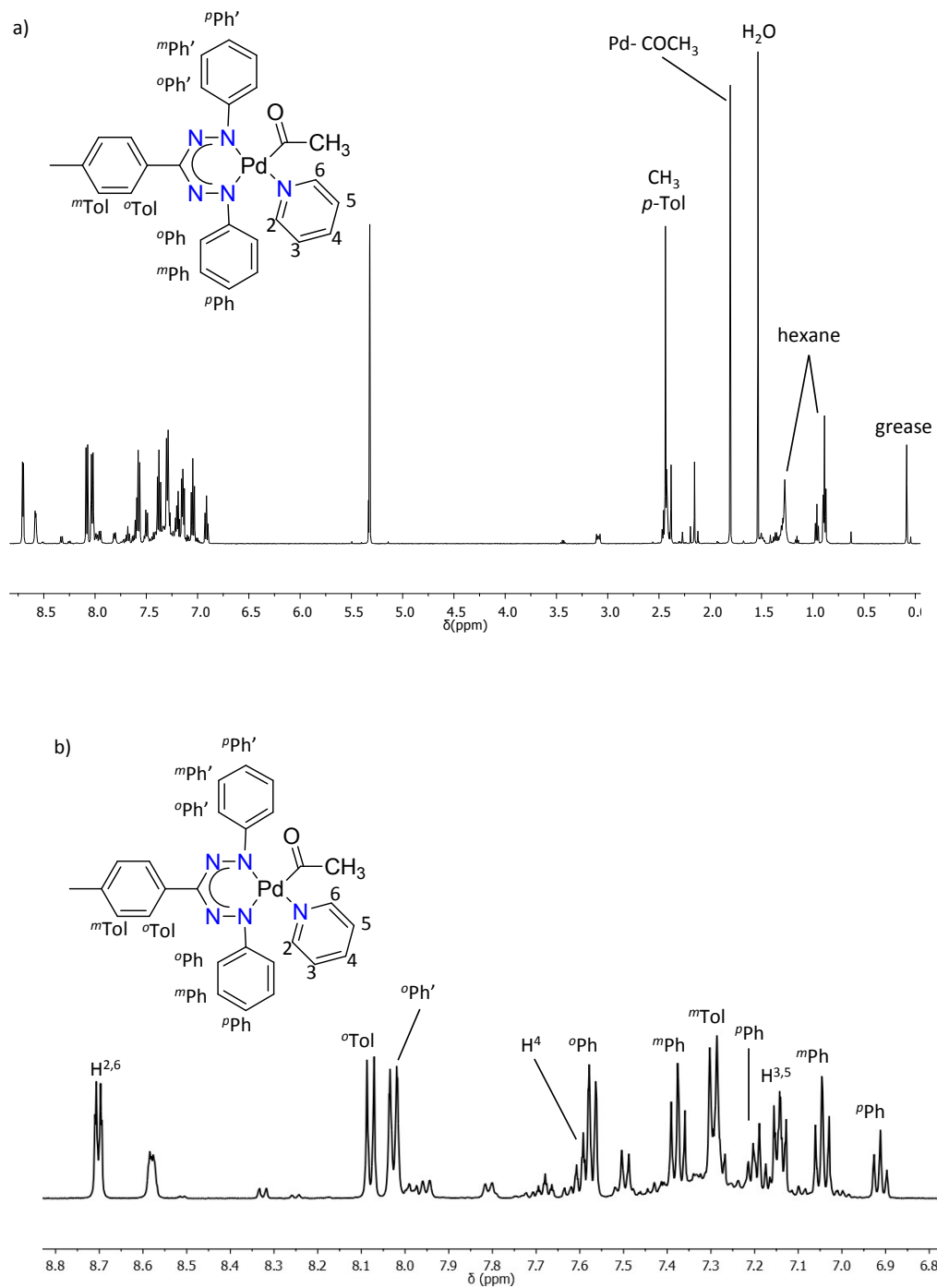


Figure S30. ¹H NMR spectrum of **8** from *in situ* NMR of **5** with CO (CD₂Cl₂, 25 °C, 400 MHz): a) full spectrum, b) aromatic region.

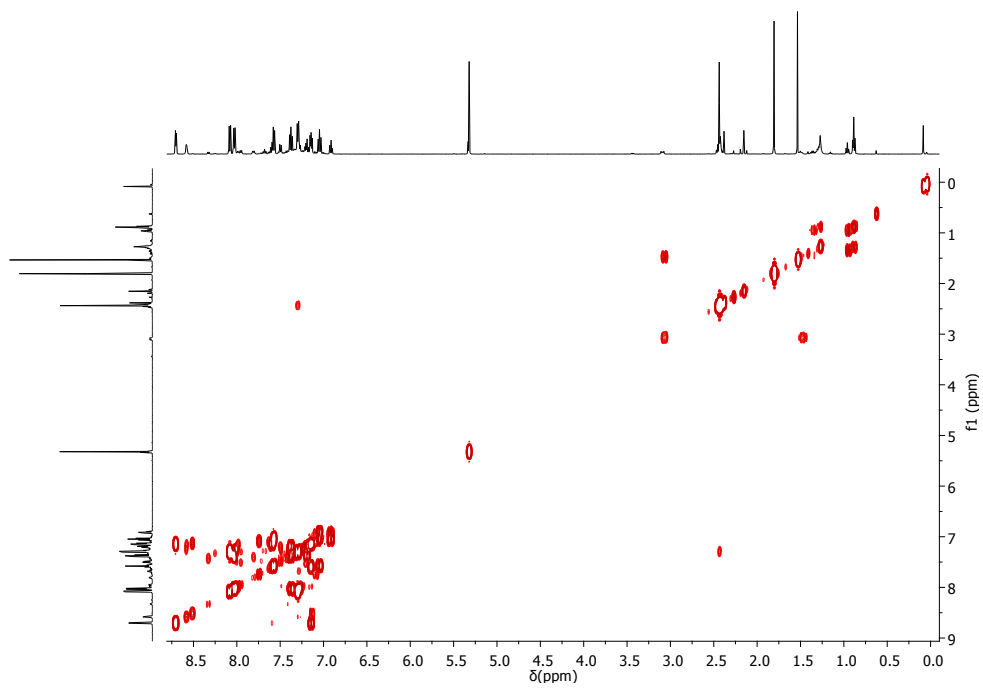


Figure S31. ^1H - ^1H gCOSY spectrum of **8** from *in situ* NMR of **5** with CO (CD_2Cl_2 , 25 °C, 400 MHz).

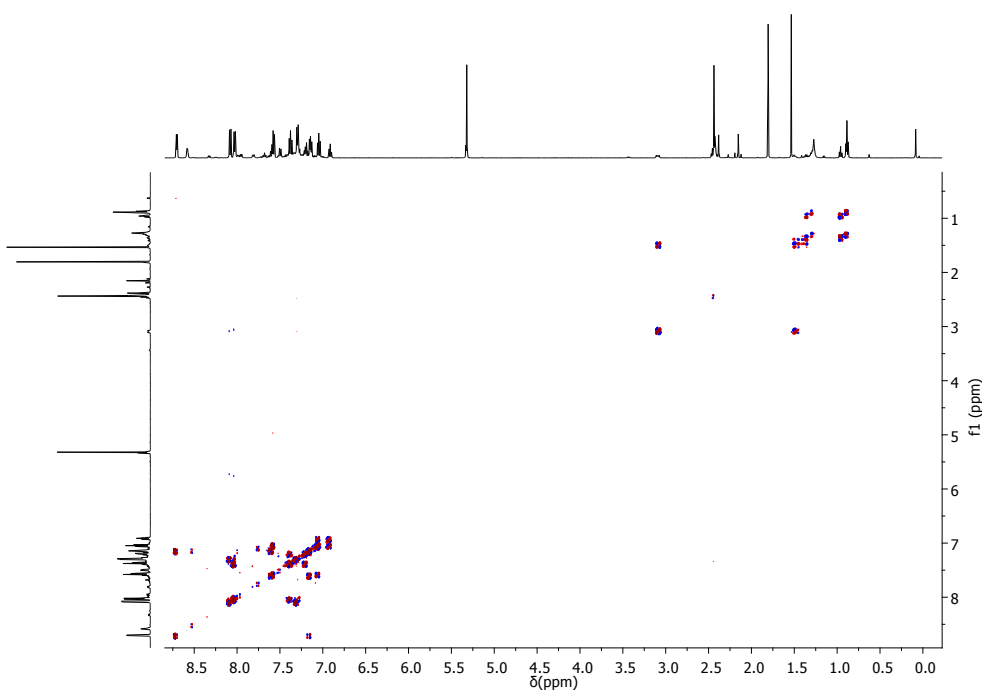


Figure S32. ^1H - ^1H gDQCOSY spectrum of **8** from *in situ* NMR of **5** with CO (CD_2Cl_2 , 25 °C, 400 MHz).

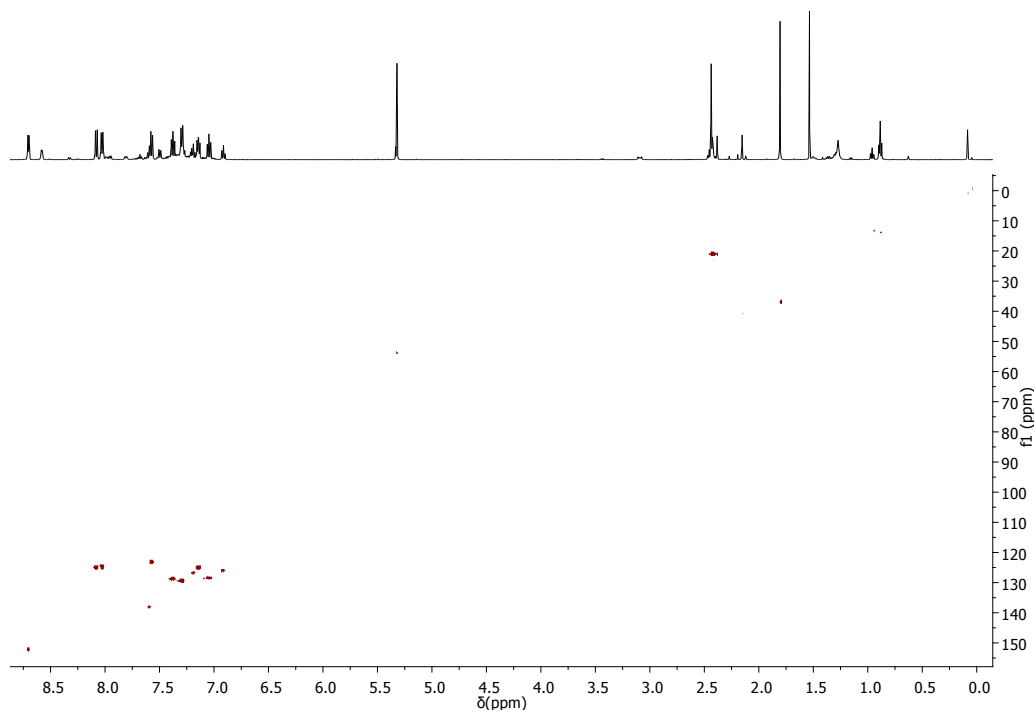


Figure S33. ^1H - ^{13}C gHSQCAD spectrum of **8** from *in situ* NMR of **5** with CO (CD_2Cl_2 , 25 °C, 400 MHz).

NMR spectra for [(1)Pd(CH(Et)CO₂Me)(py)] (9)

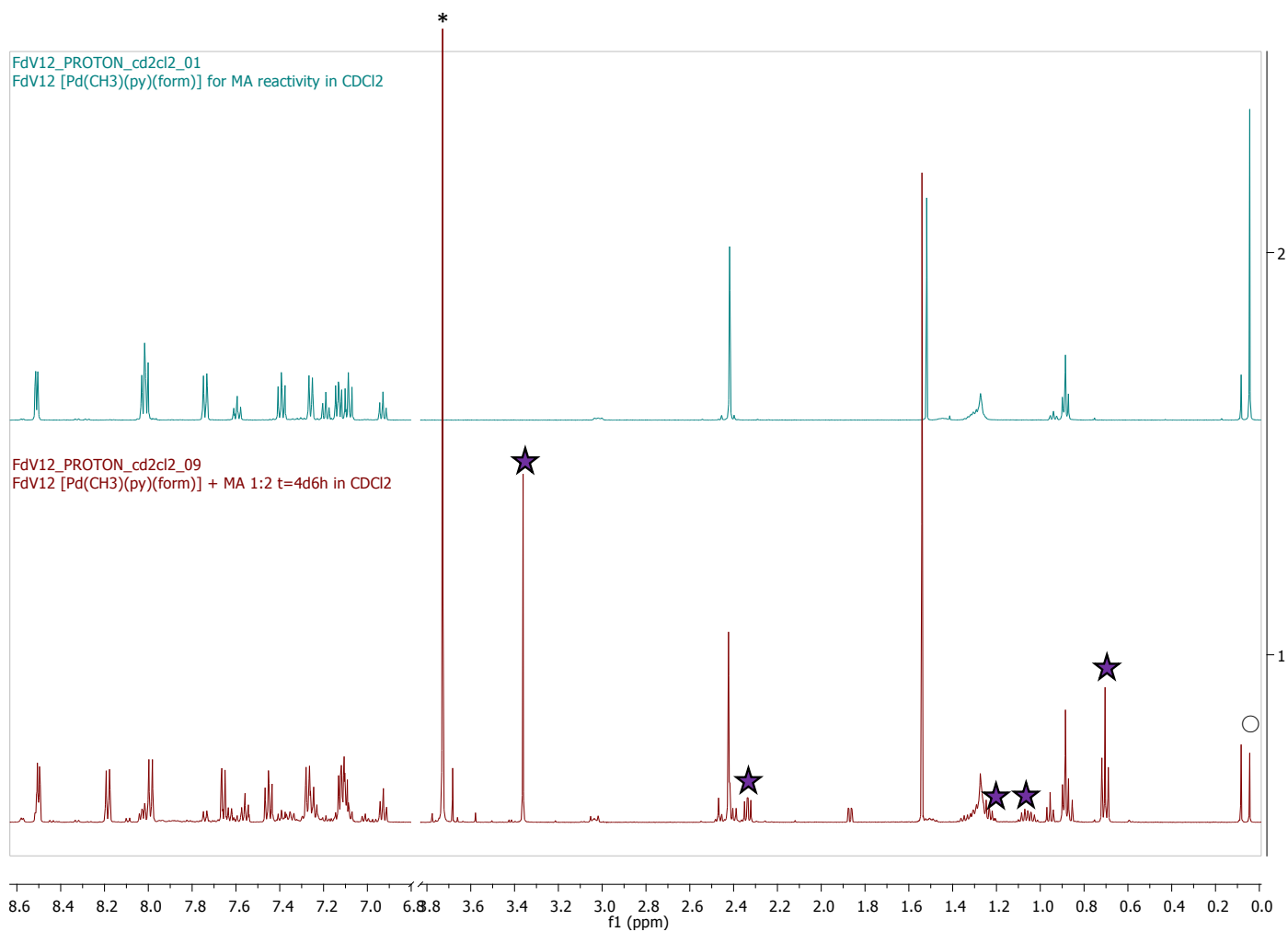


Figure S34. Top: ¹H NMR spectrum of **5** before addition of methyl acrylate. Bottom: ¹H NMR spectrum after 102 hours after addition of methyl acrylate. Area between δ 3.9-6.8 ppm not shown (contains solvent + unreacted methyl acrylate).

* -OMe peak of excess free methyl acrylate

★ New resonances that belong to the methyl acrylate insertion product

○ Pd-Me of left-over starting material

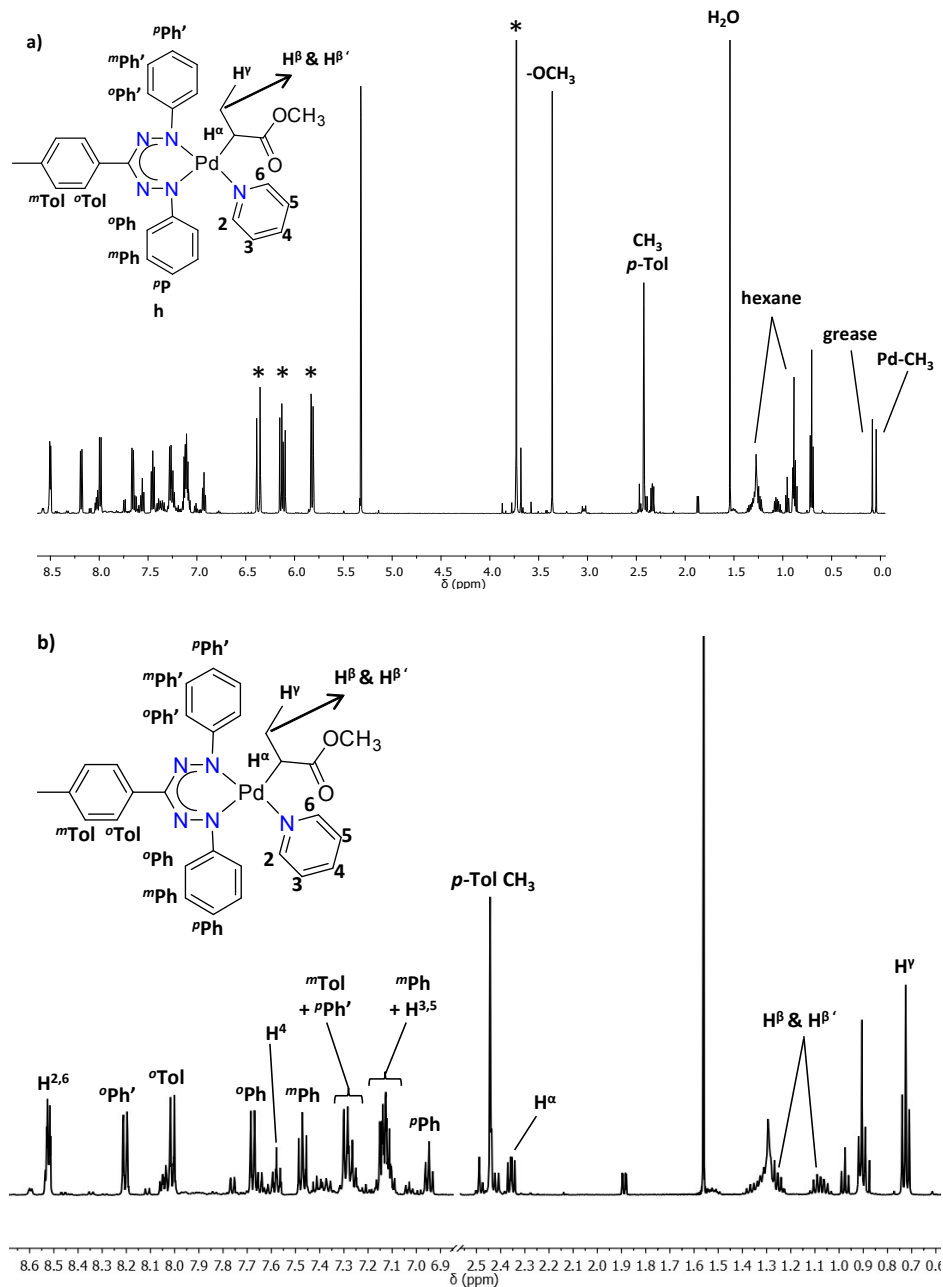


Figure S35. ^1H NMR spectrum of **9** from *in situ* NMR of **5** with 2 equivalents methyl acrylate after 102 hours of addition of methyl acrylate (500 MHz, 25 °C, CD_2Cl_2): a) full spectrum, b) aromatic region. Unreacted methyl acrylate is marked with an asterisk.

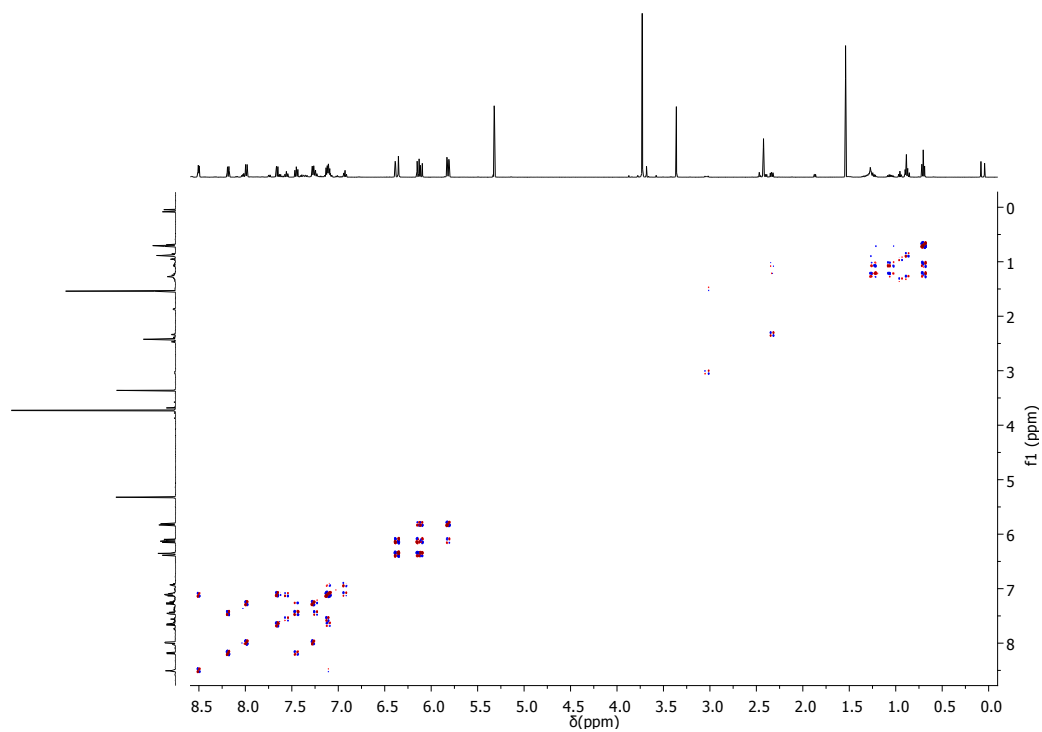


Figure S36. ^1H - ^1H DQCOSY spectrum of **9** from *in situ* NMR of **5** + 2 eq of methyl acrylate after 102 hours (500 MHz, CD_2Cl_2 , 25 °C).

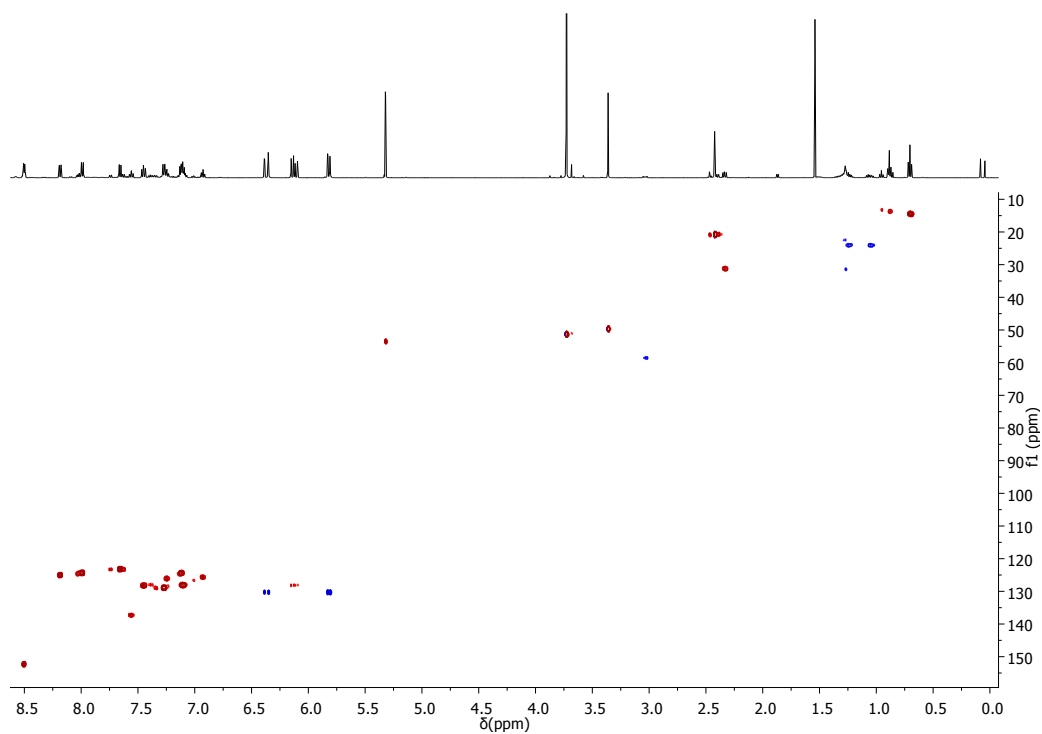


Figure S37. ^1H - ^{13}C HSQC spectrum of **9** from *in situ* NMR of **5** + 2 eq of methyl acrylate after 102 hours (500 MHz, CD_2Cl_2 , 25 °C).

***In situ* NMR reactivity studies**

***In situ* NMR reactivity of **1K** + [Pd(COD)(CH₃)Cl] in THF-*d*₈**

In a glovebox, a cold (-30 °C) solution of **1K** (0.5 eq, 11.2 mg, 1.13·10⁻² mmol) in THF-*d*₈ was added to a cold (-30 °C) solution of [Pd(COD)(CH₃)Cl] (1 eq, 6.0 mg, 2.26·10⁻² mmol) in THF-*d*₈ in a Young's NMR tube leading to a blue reaction mixture. The sample was quickly frozen in liquid nitrogen and subsequently inserted into an NMR probe pre-cooled to -40 °C. The reaction was followed for 1 day at -40 °C. The first ¹H NMR spectrum (Figure S38) shows that the starting materials are completely converted and only a trace amount of **2** is formed, which does not further increase in intensity. The aromatic region has several unidentified resonances overlapped. Species that was possible to identified are free cyclooctadiene and the palladium compound [Pd(COD)(CH₃)₂] (in THF-*d*₈, PdMe ¹H NMR: 0.22 ppm; ¹³C NMR: 3.15 ppm).¹¹ Moreover, there is a new ¹H NMR resonance at -0.05 ppm (¹³C: -5.7 ppm), which reasonably is due to a Pd-Me moiety of the putative compound [(**1**)₂PdMe].

The reaction was warmed up to +25 °C and followed for 6 days. After 24 h at room temperature the mixture is fully converted to **2**. In the ¹H NMR spectrum the resonances of **2**, free COD and [Pd(COD)(CH₃)₂] account for > 90% of the total signal intensity (Figure S38). At room temperature the [Pd(COD)(CH₃)₂] decomposed over time, and formation of a palladium mirror and methane (¹H NMR: 0.19 ppm in THF-*d*₈) and ethane (¹H NMR: 0.85 ppm in THF-*d*₈) was observed. After 6 days, compound **2** is the major species with ca. 10% of unknown byproduct(s).

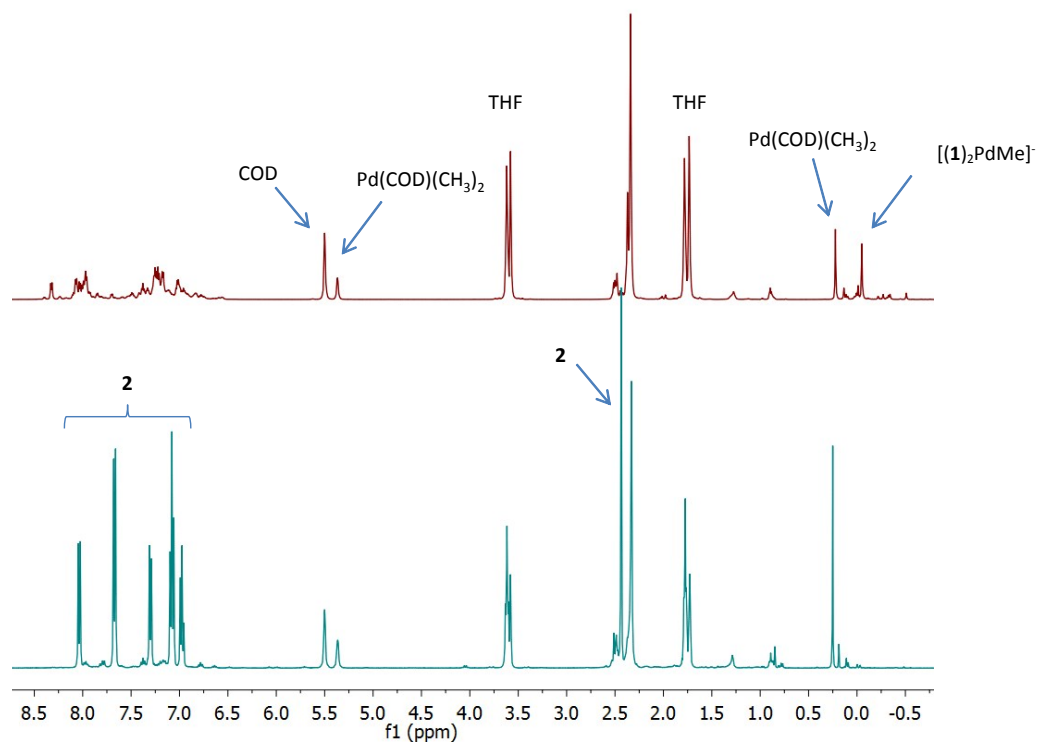


Figure S38a. ^1H NMR spectra of **1K** + $[\text{Pd}(\text{COD})(\text{CH}_3)\text{Cl}]$ in distilled $\text{THF-}d_8$, immediately after mixing at -40 $^\circ\text{C}$ (top) and after standing at room temperature for 1 day (bottom).

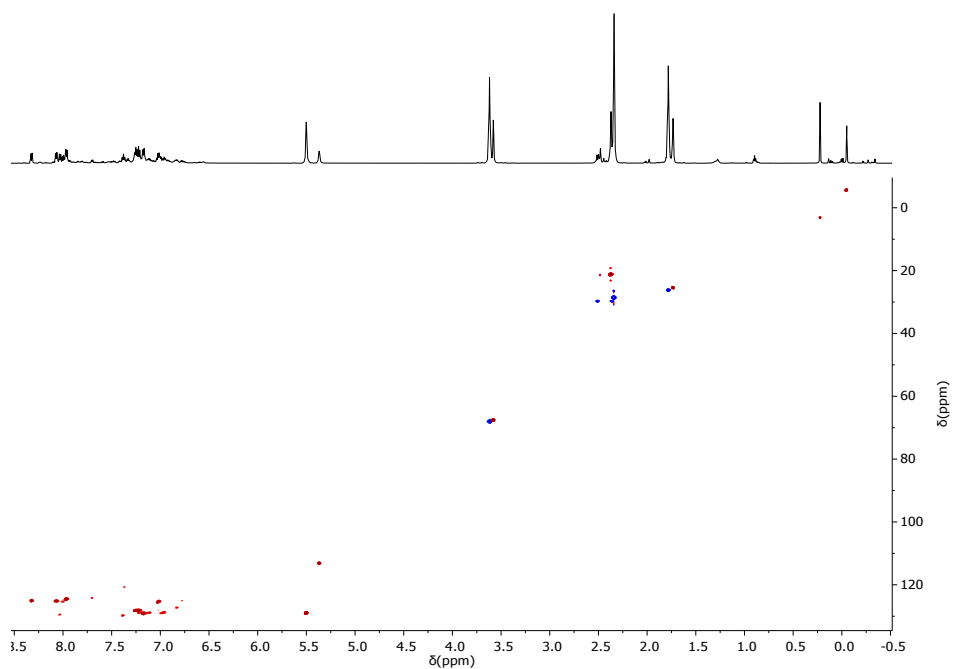


Figure S38b. ^1H - ^{13}C HSQC spectrum of **1K** + $[\text{Pd}(\text{COD})(\text{CH}_3)\text{Cl}]$, ($\text{THF-}d_8$, -40 $^\circ\text{C}$, 500 MHz).

***In situ* NMR reactivity of **1H** + [Pd(COD)(CH₃)Cl] + Et₃N in CD₂Cl₂**

To a solution of **1H** (1 eq, 2.20 mg, $7.0 \cdot 10^{-3}$ mmol) in CD₂Cl₂ in an NMR tube, [Pd(COD)(CH₃)Cl] (1 eq, 1.86 mg, $7.0 \cdot 10^{-3}$ mmol) was added as a solid to the red solution, then a ¹H NMR spectrum was recorded at +25 °C immediately after the mixing (t = 0). No reaction observed in the course of 1.5 hours. An excess of trimethylamine (1 μL) was then added via syringe. The reaction was followed over time for 3 h, which showed gradual formation of **2** and unidentified other species.

***In situ* NMR reactivity of **1H** + [Pd(COD)(CH₃)Cl] in THF-*d*₈**

In a glovebox, **1H** (1 eq, 3.8 mg, $1.2 \cdot 10^{-2}$ mmol) was added as a solid to a THF-*d*₈ solution of [Pd(COD)(CH₃)Cl] (1 eq, 3.2 mg, $1.2 \cdot 10^{-2}$ mmol) in a J. Young's NMR tube. The first ¹H NMR spectrum shows the starting materials as major species with the addition of some new minor resonances. The reaction was followed for 1 week at +25 °C. After 2 days the resonances of compound **2** start appearing, but the main species are still the starting material. After 1 week at room temperature, the reaction mixture was kept for 3 days at +60 °C, which led to a brown solution and precipitation of a blue amorphous solid (uncharacterized). The ¹H NMR spectrum shows that [Pd(COD)(CH₃)Cl] has fully reacted, and the major soluble (diamagnetic) species is compound **2**. In addition, there are also some minor unknown formazanate-containing species.

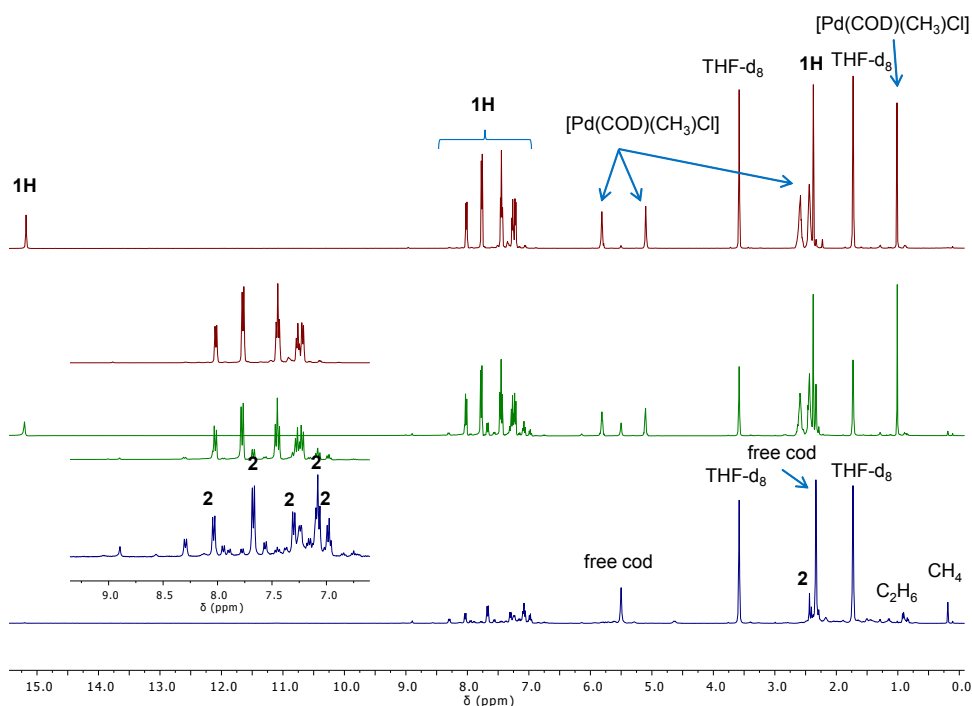


Figure S39. ¹H NMR spectrum of **1H** + [Pd(COD)(CH₃)Cl], (THF-*d*₈, 25 °C, 500 MHz) : t = 20 min (red line); t = 1 week at + 25 °C (green line), after 3 days at + 60 °C (blue line).

NMR reactivity of 4 with styrene, CO and NaBPh₄ in THF-d₈.

In a glovebox, compound **4** (3.6 mg, $5.1 \cdot 10^{-3}$ mmol) was dissolved in a J. Young's NMR tube in THF-*d*₈. To the solution was added 4 equivalents of styrene (2.9 μL, 2.6 mg, $25.3 \cdot 10^{-3}$ mmol) and the reaction was monitored via ¹H NMR spectroscopy. No changes were observed over the course of 29 hours. The solution was frozen in liquid N₂ and the J. Young's NMR tube was evacuated at the Schlenk line. Subsequently, the NMR tube was allowed to warm to room temperature and then was filled with 1 bar of CO, resulting in a color change to a darker shade of blue. The addition of CO led to the clean formation of compound **6** which was not influenced by the presence of styrene. Reaction of the in situ formed compound **6** with styrene was followed by NMR spectroscopy at -40 °C for 30 minutes, followed by another 30 minutes at RT, which did not show any insertion of styrene. Subsequently, 1 equivalent of NaBPh₄ (1.8 mg, $5.3 \cdot 10^{-3}$ mmol) was added to the J. Young's NMR tube to abstract the chloride ligand from **6**, after which the CO atmosphere was restored. The ¹H NMR spectrum taken immediately after showed decomposition of **6** to the homoleptic compound **2** and formation of palladium black was observed; no indication of olefin insertion was observed in the ¹H NMR spectra.

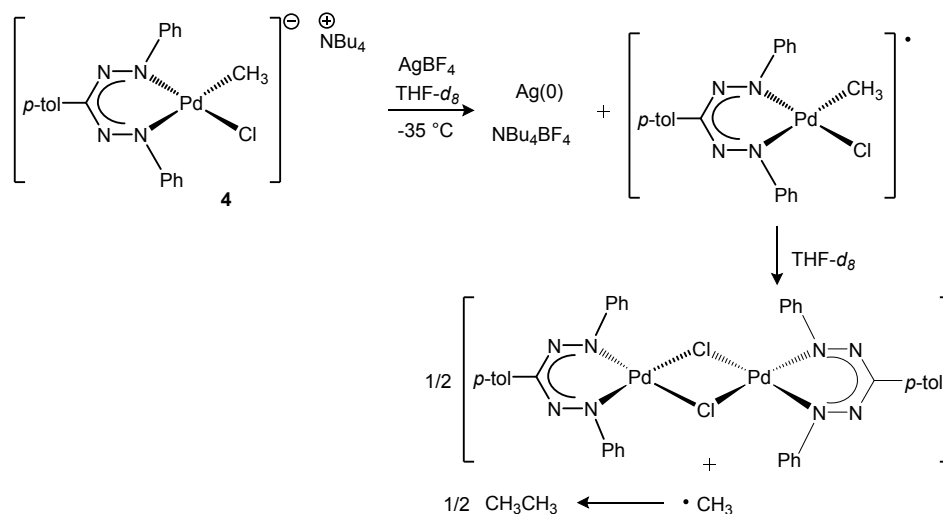
Attempted chloride abstraction from **4**

Attempts to study the formation and decomposition of the putative three-coordinate intermediate [(**1**)PdMe] were carried out by treating **4** with reagents that could abstract Cl⁻. In all cases, a solution of **4** was prepared in THF-*d*₈ and cooled to -30 °C in the glovebox freezer in a Teflon-sealed NMR tube. Subsequently, the chloride abstraction reagent was added and the sample was quickly frozen in liquid N₂ before being inserted into the cold NMR probe (at -40 °C).

Reaction of **4** with AgBF₄

Treatment of **4** with AgBF₄ proceeds rapidly at -40 °C. A ¹H NMR spectrum taken immediately upon mixing at -40 °C shows that a Pd-Me resonance is no longer observed. A new singlet at 0.85 ppm appears, which is attributed to the formation of ethane. A plausible explanation for these observations is that AgBF₄ reacts with **4** by electron transfer (rather than Cl⁻ abstraction) producing Ag⁰ and the neutral radical (**1**)PdMeCl, which subsequently results in homolysis of the Pd-Me bond to form CH₃• and the (dimeric) complex [(**1**)Pd(μ-Cl)]₂ (Scheme S1), for which there is precedent in related β-diiminate chemistry.¹² The presence of additional, very broad signals in the *in situ* ¹H NMR spectra is indicative of (unknown) paramagnetic impurities, consistent with a homolytic bond cleavage (radical) pathway. A solid sample of [(**1**)Pd(μ-Cl)]₂ was obtained by precipitation, but NMR spectroscopy showed it was contaminated with tetrabutylammonium salts (Figure S41). The amount of Bu₄N⁺ is variable between batches (based on ¹H NMR integration, see Figure S41), suggesting that the (**1**)Pd-containing fragment is not ionic, but rather the neutral complex [(**1**)Pd(μ-Cl)]₂.

Scheme S1. Proposed reaction sequence for reaction of **4** with AgBF₄ in THF-*d*₈.



Experimental procedure for *in situ* NMR reaction of 4 with AgBF₄ in THF-*d*₈. In glovebox, to a cold (-30 °C) solution of 4 (5.5 mg, 8.0·10⁻³ mmol) in THF-*d*₈, in a Young's NMR tube, AgBF₄ (excess) was added as a solid. The sample was quickly frozen in liquid nitrogen and subsequently inserted into an NMR probe pre-cooled to -40 °C. The reaction was followed for 1 day at -40 °C and then was warmed up to +25 °C. The volatiles were removed and the solid was redissolved in THF-*d*₈ to confirm the disappearance of the peak of ethane at 0.85 ppm. Filtration of a THF through a 0.2 μm filter, followed by slow diffusion of hexane afforded a blue powder (the putative complex [(1)Pd(μ-Cl)]₂), as a mixture with a Bu₄N⁺ salt (the ratio between [(1)Pd(μ-Cl)]₂ and Bu₄N⁺ is dependent on the batch, see Figure S41).

[(1)Pd(μ-Cl)]₂ ¹H NMR (400 MHz, THF-*d*₈, 25 °C): δ 8.40 (d, 8H, Ph *o*-CH), 7.94 (d, 4H *p*-tolyl *o*-CH), 7.53 (t, 8H Ph *m*-CH), 7.37 (t, 4H Ph *p*-CH), 7.28(d, 4H *p*-tolyl *m*-CH) 2.40 (s, 6H, *p*-tolyl CH₃) ppm.

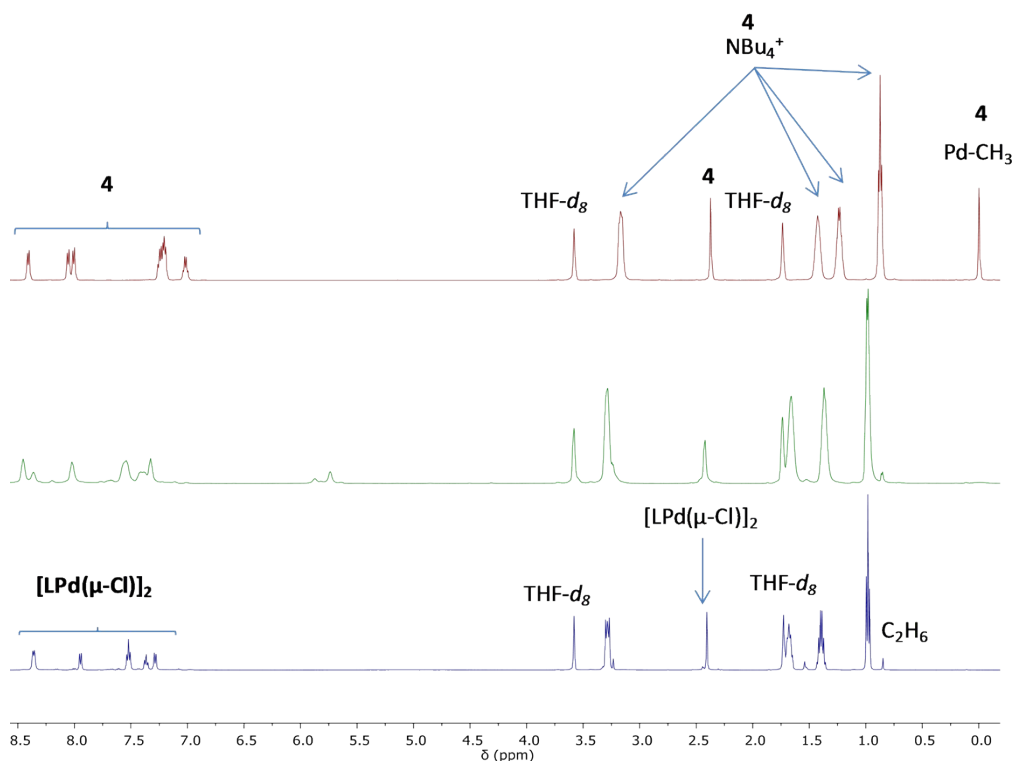


Figure S40. ¹H NMR spectrum of 4 (THF-*d*₈, 500 MHz): at -40 °C (red line), + AgBF₄ at -40 °C (green line), + AgBF₄ at +25 °C (blue line).

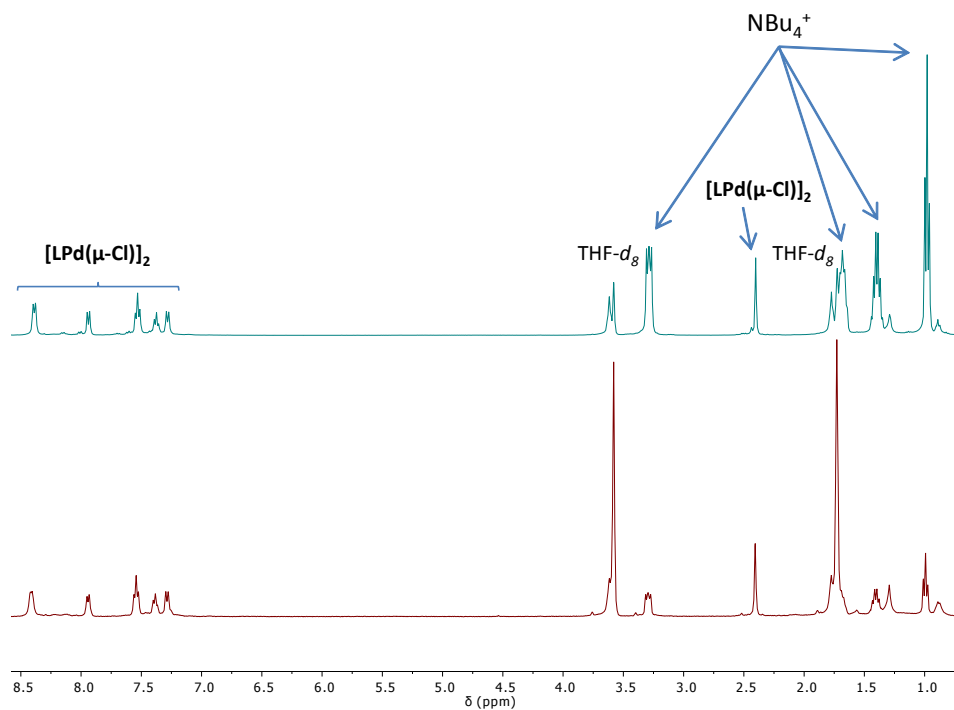


Figure S41. ^1H NMR spectrum of the isolated solid, $[(\mathbf{1})\text{Pd}(\mu\text{-Cl})]_2$, from reaction of **4** with AgBF_4 ($\text{THF-}d_8$, 400 MHz; bottom and top spectra show different batches highlighting the varying amount of Bu_4N^+ present).

Reaction of **4** with NaBPh₄.

The analogous reaction of **4** with NaBPh₄ does not proceed at -40 °C, but increasing the temperature gave a complicated mixture in which **2** is ultimately the major product in solution (Scheme S2, Figure S42). However, also the formation of a palladium mirror is observed, and a white solid is precipitated (NaCl).

Scheme S2. Proposed reaction sequence for *in situ* NMR reactivity of **4** + NaBPh₄ in THF-*d*₈.



Experimental procedure for *in situ* NMR reaction of **4** with NaBPh₄ in THF-*d*₈.

In a glovebox, to a cold (-30 °C) solution of **4** (1 eq, 5.5 mg, 8.0·10⁻³ mmol) in THF-*d*₈, in a Young's NMR tube, NaBPh₄ (1 eq, 2.7 mg, 8.0·10⁻³ mmol) was added as a solid. The sample was quickly frozen in liquid nitrogen and subsequently inserted into an NMR probe pre-cooled to -40 °C. The reaction was followed for 2 h at -40 °C (no reaction was observed), for 2 days at +25 °C and then the sample was warmed up to +75 °C for 5 days after which a dark green-brownish solution was observed together with formation of a Pd(0) mirror and precipitation of a white solid.

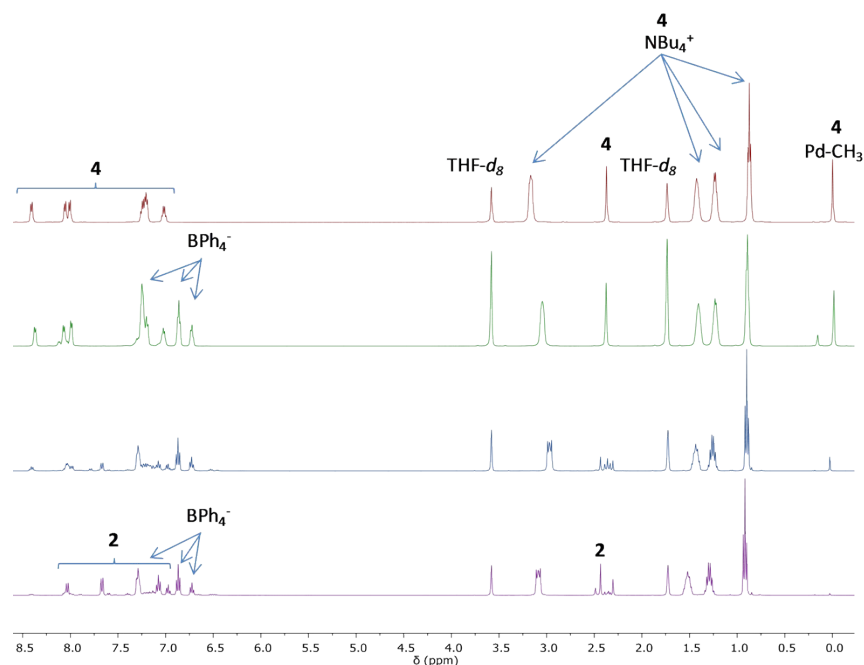
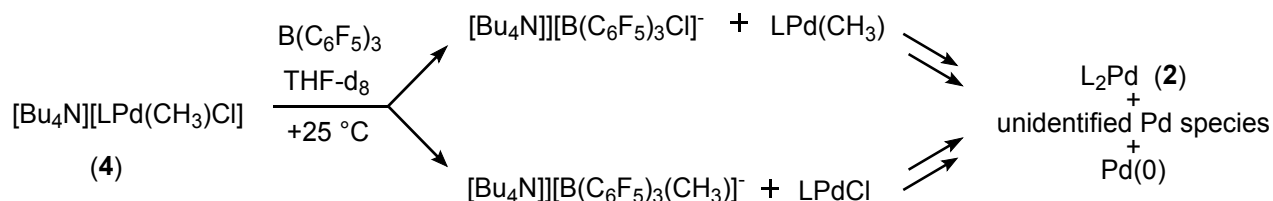


Figure S42. ¹H NMR spectrum of **4** (THF-*d*₈, 500 MHz): at -40 °C (red line), + NaBPh₄ at -40 °C t= 1h 30 min (green line), + NaBPh₄ at +25 °C t=1 day (blue line), + NaBPh₄ after heating the sample at +75 °C for 5 days, spectrum recorded at +25 °C (blue line).

Reaction of **4** with $B(C_6F_5)_3$

Chloride abstraction using the Lewis acid $B(C_6F_5)_3$ at $-40\text{ }^\circ\text{C}$ immediately forms **2** as the major product in solution (Scheme S3). Concomitantly, a significant amount of blue solid is precipitated which was insoluble in common (organic) solvents including MeOH, DMSO, mineral acid and the ionic liquid imidazolium salt. ^{19}F NMR analysis of the brown supernatant solution shows that the borane is converted to a mixture of chloro- and methylborate ($[B(C_6F_5)_3Cl]^-$ and $[B(C_6F_5)_3Me]^-$, assigned by comparison to literature NMR data)¹³ in a ratio of ca. 2:1, respectively (Figure S44).

Scheme S3. Proposed reaction sequence for *in situ* NMR reactivity of **4** + $B(C_6F_5)_3$ in THF- d_8 .



In situ NMR reactivity of **4** with $B(C_6F_5)_3$ in THF- d_8

In a glovebox, to a solution of $B(C_6F_5)_3$ (1 eq, 4.1 mg, $8.0 \cdot 10^{-3}$ mmol) in THF- d_8 , in a Young's NMR tube, **4** (1 eq, 5.5 mg, $8.0 \cdot 10^{-3}$ mmol) was added as a solid, leading to a dark brown reaction mixture and precipitation of a dark blue solid. The reaction was followed via ^1H , ^{19}F , ^{11}B NMR spectroscopy at $+25\text{ }^\circ\text{C}$. The ^1H NMR spectrum recorded after 20 min shows that compound **4** has almost completely reacted, leading to compound **2** as major species in addition to some traces amount of unidentified formazanate species and free ligand. In addition to this, in the aliphatic region the resonances of NBu_4^+ (^1H NMR: 3.21, 1.64, 1.37, 0.97 ppm, in THF- d_8) and of methane (^1H NMR: 0.19 ppm in THF- d_8) and ethane (^1H NMR: 0.85 ppm in THF- d_8) are present. The ^{19}F and ^{11}B NMR spectra recorded after 20 min show a mixture of $B(C_6F_5)_3$, $[B(C_6F_5)_3Cl]^-$ and $[B(C_6F_5)_3CH_3]^-$.

$B(C_6F_5)_3$: ^{19}F NMR (376 MHz, THF- d_8 , $25\text{ }^\circ\text{C}$): -131.8 (6H, d, *o*-F), -156.5 (3H, t, *p*-F), -163.3 (6H, t, *m*-F) ppm. ^{11}B NMR (128 MHz, THF- d_8 , $25\text{ }^\circ\text{C}$): + 4.4 ppm.

$[B(C_6F_5)_3Cl]^-$: ^{19}F NMR (376 MHz, THF- d_8 , $25\text{ }^\circ\text{C}$): -130.4 (6H, m, *o*-F), -162.5 (3H, t, *p*-F), -166.8 (6H, m, *m*-F) ppm. ^{11}B NMR (128 MHz, THF- d_8 , $25\text{ }^\circ\text{C}$): -7.6 ppm.

[B(C₆F₅)₃CH₃]⁻: ¹H NMR (400 MHz, THF-*d*₈, 25 °C): 0.5 (br, B-CH₃) ppm. ¹⁹F NMR (376 MHz, THF-*d*₈, 25 °C): -130.9 (6H, m, *o*-F), -165.2 (3H, t, *p*-F), -167.3 (6H, m, *m*-F) ppm. ¹¹B NMR (128 MHz, THF-*d*₈, 25 °C): - 14.9 ppm.

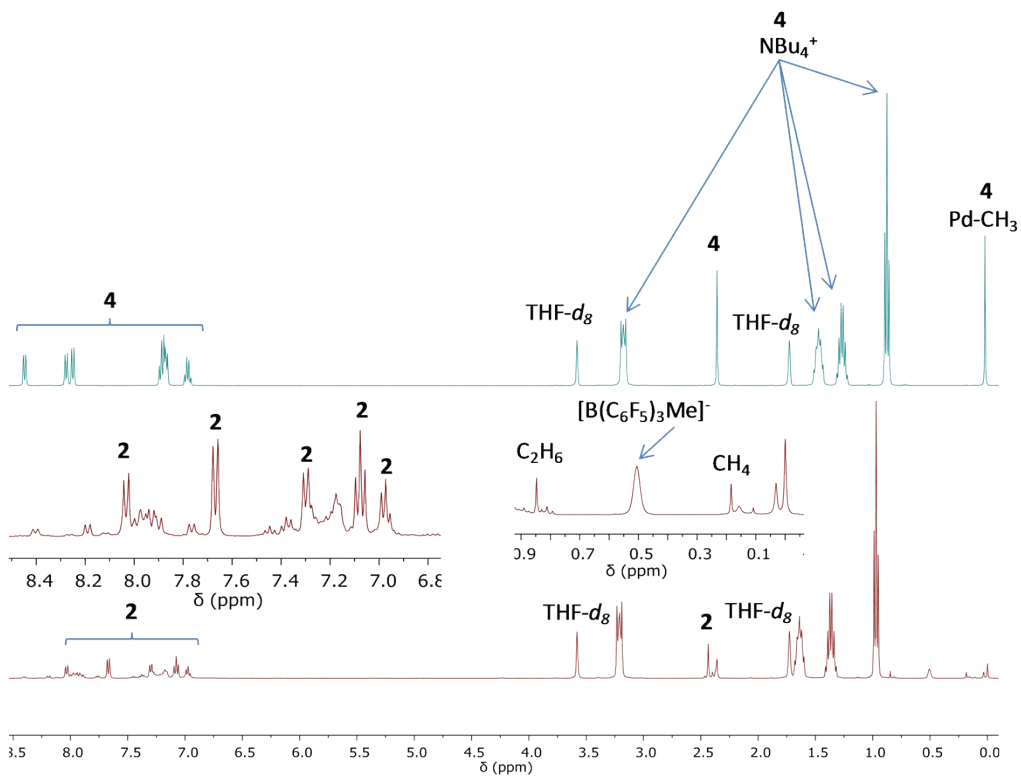


Figure S43. ¹H NMR spectrum of **4** (THF-*d*₈, 400 MHz) (top), + B(C₆F₅)₃ t= 20 min (bottom).

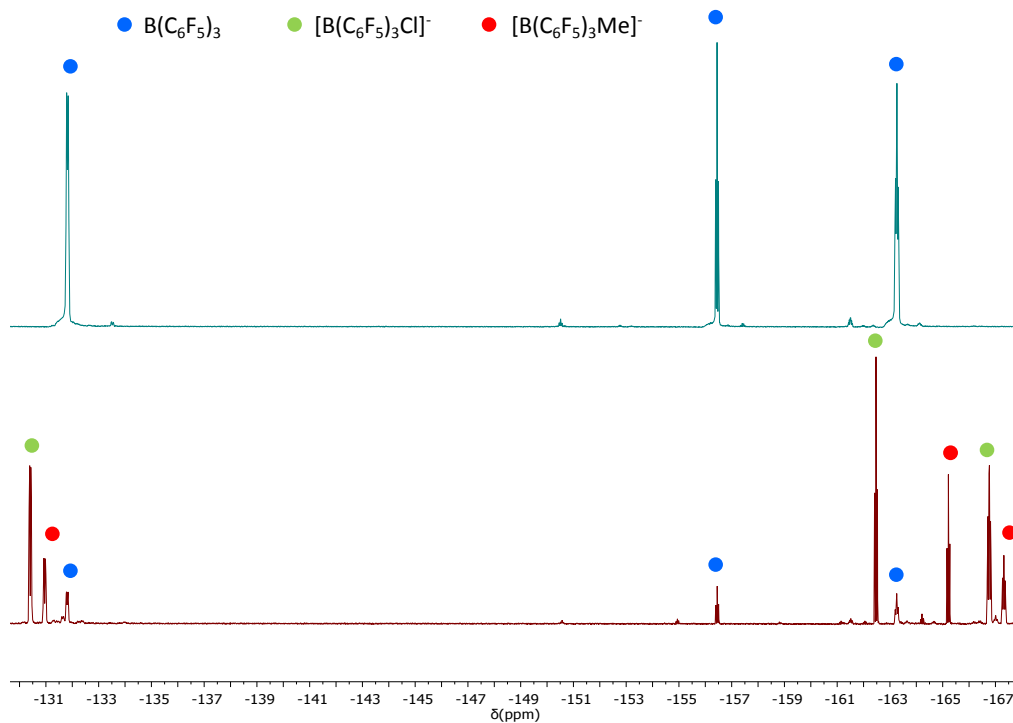


Figure S44. ^{19}F NMR spectrum ($\text{THF-}d_8$, 376 MHz) of: $\text{B}(\text{C}_6\text{F}_5)_3$ (top), **4** + $\text{B}(\text{C}_6\text{F}_5)_3$ $t = 20$ min (bottom).

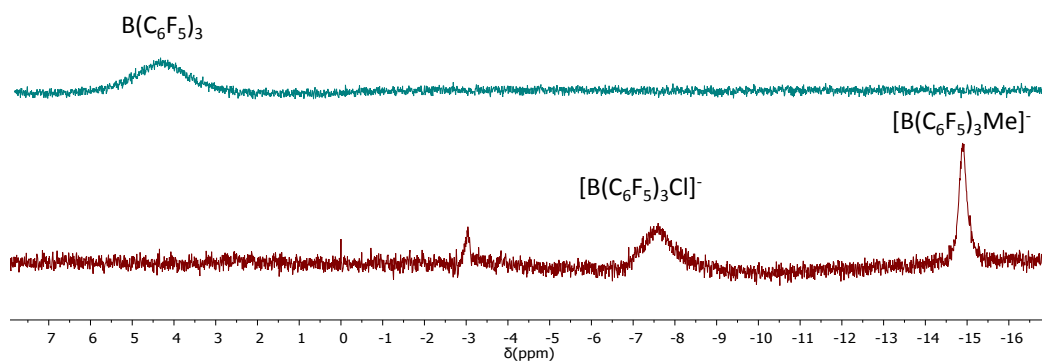


Figure S45. ^{11}B NMR spectrum ($\text{THF-}d_8$, 128 MHz) of: $\text{B}(\text{C}_6\text{F}_5)_3$ (THF adduct, top), **4** + $\text{B}(\text{C}_6\text{F}_5)_3$ $t = 20$ min (bottom).

UV-Vis absorption spectra

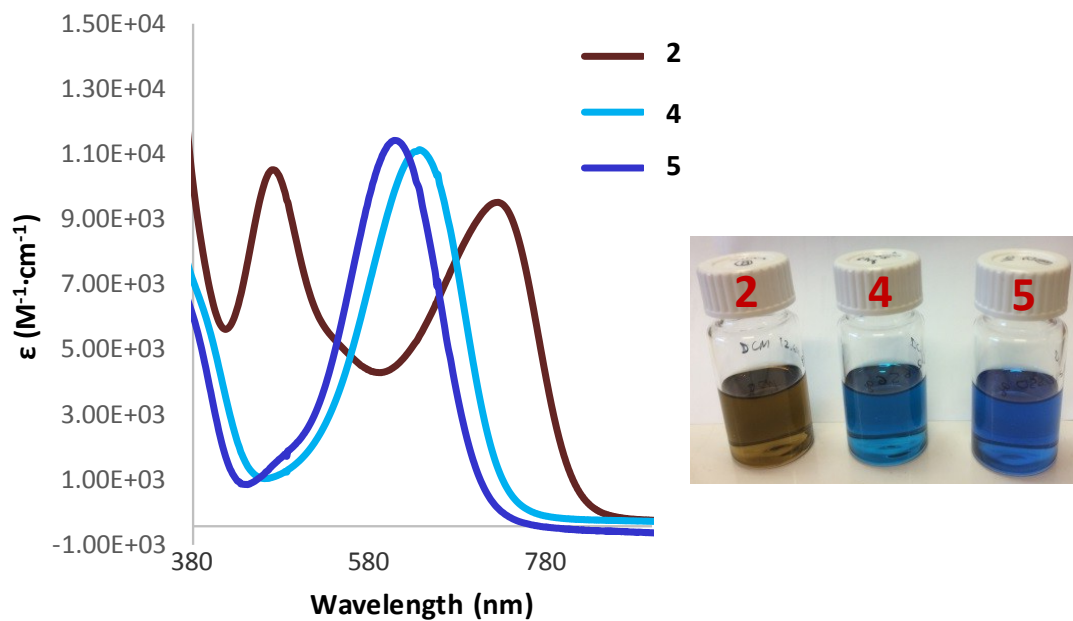


Figure S46. Left: UV-Vis absorption spectra of compounds **2**, **4**, and **5** in CH_2Cl_2 . Right: Physical appearance of the CH_2Cl_2 solutions of compounds **2**, **4**, and **5**.

Cyclic voltammetry data

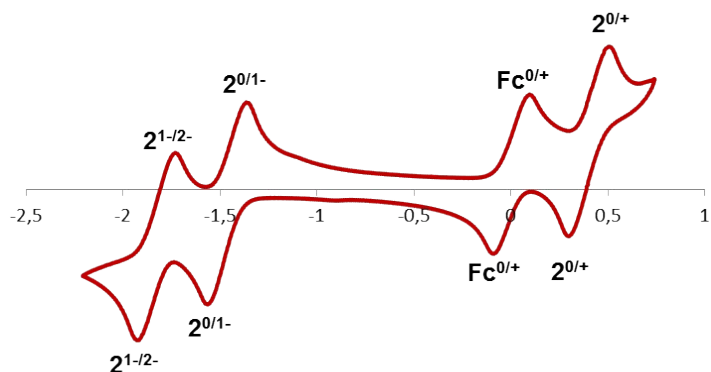


Figure S47. Cyclic voltammogram of compound **2** (ca. 1.50 mM solution of **2** in THF; 0.1 M $[nBu_4N][PF_6]$ electrolyte; scan rate = $0.5\text{ V}\cdot\text{s}^{-1}$).

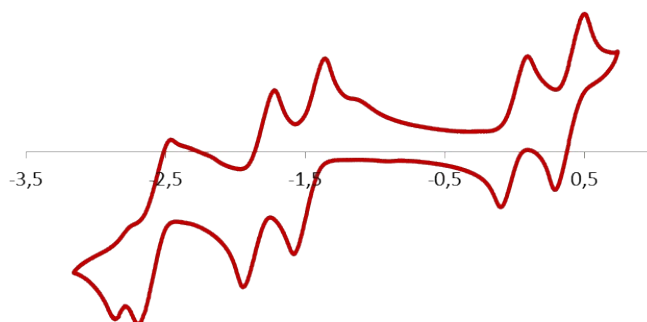


Figure S48. Cyclic voltammogram of compound **2**, larger window (ca. 1.50 mM solution of **2** in THF; 0.1 M $[nBu_4N][PF_6]$ electrolyte; scan rate = $0.5\text{ V}\cdot\text{s}^{-1}$).

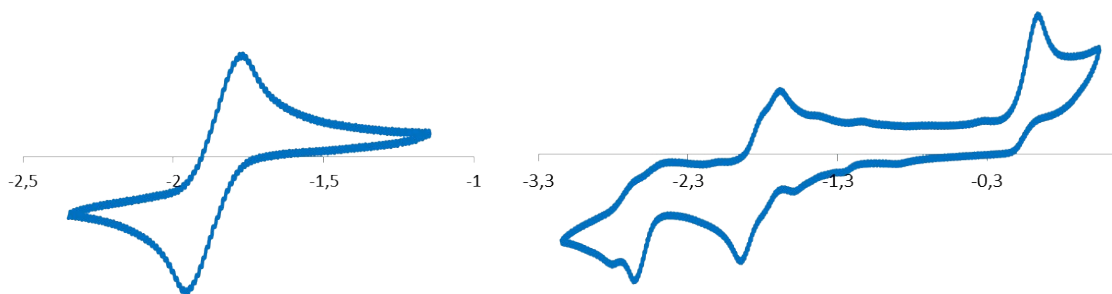


Figure S49. Cyclic voltammograms of compound **4** (ca. 1.50 mM solution of **4** in THF; 0.1 M $[nBu_4N][PF_6]$ electrolyte; scan rate = $0.1\text{ V}\cdot\text{s}^{-1}$).

Attempted catalytic reactions

2,2,2-trifluoroethanol (TFE) was used without further purification. Carbon monoxide (CP grade 99.9%) supplied by SIAD, styrene (99%, with 4-*tert*-butylcatechol), 4-methylstyrene (99%, with 4-*tert*-butylcatechol) supplied by Aldrich were used as received. 1,4-benzoquinone was used as oxidant, to increase the stability of the catalyst, limiting the decomposition to inactive palladium metal.¹⁴

CO/styrene copolymerization reactions at 1 bar

All experiments were performed at atmospheric CO pressure in a three-necked, thermostated, 75 mL glass reactor equipped with a magnetic stirrer. After establishment of the reaction temperature, complex **2** ($1.27 \cdot 10^{-5}$ mol), 1,4-benzoquinone ([BQ]/[Pd]=5), styrene (10 mL) and TFE (20 mL) were added. CO was bubbled through the solution for 10 min; afterwards two 4 L balloons previously filled with CO were connected to the reactor. After the desired time, the reaction mixture was poured into 100 mL of methanol. Since no precipitation was observed the solvent was removed under *vacuum* and the solid was analyzed via NMR spectroscopy, which showed that **2** was recovered unchanged. Catalytic reactions using **4** resulted in free ligand and **2** at the end of the reaction.

CO/Vinyl arene Copolymerization Reactions at high CO pressure.

All experiments were carried out in a stainless steel autoclave (150 mL), equipped with a Teflon liner, magnetic stirrer, heating mantle, and temperature controller. Complex **2**, the vinyl arene, 1,4-benzoquinone, and the solvent were placed in the reactor. CO was bubbled through the solution for 10 min; afterwards the reactor was pressurized at the desired pressure and heated. After 24 h, the reactor was vented, and methanol (200 mL) was added. The reaction mixture was poured into 100 mL of methanol. Since no precipitation was observed the solvent was removed under *vacuum* and the solid was analyzed via NMR spectroscopy, which showed that **2** was recovered unchanged.

Table S1. CO/vinyl arene copolymerization.^[a]

Entry	Polar monomer	Precatalyst	T (°C)	P _{CO} (atm)
1 ^[b]	Styrene	2	30	1
2 ^[b]	Styrene	2	45	1
3	Styrene	2	30	10
4	Styrene	2	30	20
5	Styrene	2	50	20
6	Styrene	2	70	20
7	4-Me-Styrene	2	70	20
8 ^[b]	Styrene	4	30	1
9 ^[b,c]	Styrene	4	30	1

^[a]Reaction conditions: $n_{\text{Pd}} = 1.91 \times 10^{-5}$ mol, TFE: V = 30 mL, vinyl arene V = 15 mL; [styrene]/[Pd] = 6800; [4-Me-styrene]/[Pd] = 5900; [BQ]/[Pd] = 5; t = 24 h.

^[b]Reaction conditions: $n_{\text{Pd}} = 1.91 \times 10^{-5}$ mol, TFE: V = 20 mL, vinyl arene V = 10 mL; [styrene]/[Pd] = 6800; [4-Me-styrene]/[Pd] = 5900; [BQ]/[Pd] = 5; t = 24 h.

^[c]With AgPF₆ as additive for chloride abstraction.

References

1. J. B. Gilroy, M. J. Ferguson, R. McDonald, B. O. Patrick and R. G. Hicks, *Chem. Commun.*, 2007, 126-128.
2. R. Travieso-Puente, M.-C. Chang and E. Otten, *Dalton Trans.*, 2014, **43**, 18035-18041.
3. R. E. Rulke, J. M. Ernsting, A. L. Spek, C. J. Elsevier, P. W. N. M. van Leeuwen and K. Vrieze, *Inorg. Chem.*, 1993, **32**, 5769-5778.
4. Collaborative Computational Project Number 4, *Acta Cryst. D*, 1994, **50**, 760-763.
5. Z. Otwinowski and W. Minor, in *International Tables for Crystallography Volume F: Crystallography of biological macromolecules*, eds. M. G. Rossmann and E. Arnold, Springer Netherlands, Dordrecht, 2001, pp. 226-235.
6. G. Sheldrick, *Acta Cryst. A*, 2008, **64**, 112-122.
7. Bruker., *APEX3, SAINT and SADABS. Bruker AXS Inc., Madison, Wisconsin, USA.*, 2016.
8. G. Sheldrick, *Acta Cryst. A*, 2015, **71**, 3-8.
9. G. Sheldrick, *Acta Cryst. C*, 2015, **71**, 3-8.
10. M. J. Frisch, G. W. Trucks, H. B. Schlegel, G. E. Scuseria, M. A. Robb, J. R. Cheeseman, G. Scalmani, V. Barone, B. Mennucci, G. A. Petersson, H. Nakatsuji, M. Caricato, X. Li, H. P. Hratchian, A. F. Izmaylov, J. Bloino, G. Zheng, J. L. Sonnenberg, M. Hada, M. Ehara, K. Toyota, R. Fukuda, J. Hasegawa, M. Ishida, T. Nakajima, Y. Honda, O. Kitao, H. Nakai, T. Vreven, J. A. Montgomery Jr., J. E. Peralta, F. Ogliaro, M. J. Bearpark, J. Heyd, E. N. Brothers, K. N. Kudin, V. N. Staroverov, R. Kobayashi, J. Normand, K. Raghavachari, A. P. Rendell, J. C. Burant, S. S. Iyengar, J. Tomasi, M. Cossi, N. Rega, N. J. Millam, M. Klene, J. E. Knox, J. B. Cross, V. Bakken, C. Adamo, J. Jaramillo, R. Gomperts, R. E. Stratmann, O. Yazyev, A. J. Austin, R. Cammi, C. Pomelli, J. W. Ochterski, R. L. Martin, K. Morokuma, V. G. Zakrzewski, G. A. Voth, P. Salvador, J. J. Dannenberg, S. Dapprich, A. D. Daniels, Ö. Farkas, J. B. Foresman, J. V. Ortiz, J. Cioslowski and D. J. Fox, *Gaussian 09, Revision D.01*, 2009.
11. Carrying out the reaction in CD₂Cl₂ also results in formation of [Pd(COD)(CH₃)₂]: identical NMR shifts as those reported by Jordan and co-workers are observed.
12. A. Hadzovic and D. Song, *Organometallics*, 2008, **27**, 1290-1298.
13. G. Bellachioma, G. Cardaci, E. Foresti, A. Macchioni, P. Sabatino and C. Zuccaccia, *Inorg. Chim. Acta*, 2003, **353**, 245-252.
14. B. Milani, A. Anzilutti, L. Vicentini, A. Sessanta o Santi, E. Zangrando, S. Geremia, G. Mestroni, *Organometallics*, 1997, **16**, 5064-5075.